

Approximation-free control based on the bioinspired reference model for suspension systems with uncertainty and unknown nonlinearity

Xiaoyan Hu, Guilin Wen, Shan Yin, Zhao Tan, and Zebang Pan

Abstract—Uncertainty and unknown nonlinearity are often inevitable in the suspension systems, which were often solved using fuzzy logic system (FLS) or neural networks (NNs). However, these methods are restricted by the structural complexity of the controller and the huge computing cost. Meanwhile, the estimation error of such approximators is affected by adopted adaptive laws and learning gains. Thus, in view of the above problem, this paper proposes the approximation-free control based on the bioinspired reference model for a class of uncertain suspension systems with unknown nonlinearity. The proposed method integrates the superior vibration suppression of the bioinspired reference model and the structural advantage of the prescribed performance function (PPF) in approximation-free control. Then, the vibration suppression performance is improved, the calculation burden is relieved, and the transient performance is improved, which is analyzed theoretically in this paper. Finally, the simulation results validate the approach, and the comparisons show the advantages of the proposed control method in terms of good vibration suppression, fast convergence, and less calculation burden.

Index Terms—Approximation-free, bioinspired reference model, suspension system, uncertainty, unknown nonlinearity

I. INTRODUCTION

THE suspension system is one of the important components in vehicles to ensure passengers' ride comfort and safety by isolating the vibration from road excitation and adapting to the complexity of tough roads. Generally, there are three types of suspension systems: passive suspension, semi-active suspension, and active suspension. Passive suspensions absorb vibration mainly through dampers and springs installed inside, passively. The contradictory ride comfort requirements and handling stability cannot be satisfied simultaneously due

to the fixed system parameters. Thus, the semi-active suspension is proposed to improve adaptation by adjusting the damper and spring force, but it cannot be controlled optimally according to external input. Compared to passive and semi-active suspension, active suspensions isolate vibration and offer more comfort effectively and flexibly by producing an active force, whose design and analysis get the most attention from researchers. Due to the simple structure, linear active suspension models have been studied for decades. Some feedback control schemes, such as feedback control [1]–[4] and H_∞ control method with LMI (Linear matrix inequality) [2], [3], [5], [6], were implemented smoothly to achieve significant results in these models. However, most of the existing results focused on linear active suspension systems with delay or uncertainty in recent works. Besides, the main form of control methods is feedback gain structure essentially. Furthermore, some linear control methods cannot be further applied in nonlinear systems. Thus, many researchers are investigating nonlinear active suspension system, which has more realistic value and engineering applicability. Various synthetical control methods are widely studied to address the nonlinearity in active suspension systems. In Ref. [7], considering the highly complex nonlinearity in the hydraulic actuator, the higher-order terminal sliding mode control was established to stabilize uncertain suspension systems. Adaptive backstepping control was applied to uncertain nonlinear suspension systems considering input delay [8] and hard constraints [9]. The adaptive control was established in Ref. [10] with synchronization control to synchronize the height of four suspensions of the vehicle.

Owing to the diversity of passengers, measurement technique limitation, and inherent dynamic property, uncertainty and unknown nonlinearity are inevitable in suspension systems. In order to tackle these issues, approximation methods, such as neural networks (NNs) and fuzzy logic systems (FLS) are extensively investigated by cooperating different control strategies. In Ref. [11], with the assistance of NNs approximating uncertain dynamics, the adaptive finite-time control was proposed. The stability and ride comfort of the half suspension system could be achieved during a finite time. For a class of uncertain suspension systems with the time-varying vertical displacement and speed constraints, the adaptive controller

Xiaoyan Hu, Shan Yin, Zhao Tan and Zebang Pan are with State Key Laboratory of Advanced Design and Manufacture for Vehicle Body, Hunan University, Changsha, Hunan 410082, China. (e-mail: nicole0106@hnu.edu.cn; shan.yin@hnu.edu.cn; tanzhao@hnu.edu.cn; zbpan@hnu.edu.cn)

Guilin Wen is with: 1 State Key Laboratory of Advanced Design and Manufacture for Vehicle Body, Hunan University, Changsha, Hunan 410082, China. 2 School of Mechanical Engineering, Yanshan University, Qinhuangdao, Hebei 066004, China (e-mail: glwen@hnu.edu.cn)

based on the NNs approximator was established in Ref. [12]. Considering the limitation of communication resources, the event-trigger controller with NNs approximating the unknown term was adopted to release the communication burden on electromagnetic actuator to the controller [13]. The approximator FLS generally cooperates with different control methods including adaptive backstepping control and sliding mode control for a class of suspension systems with nonlinearity or uncertainty. In Ref. [14], the suspension system's input delay and unknown nonlinearity were considered and handled by compensation scheme and FLS, respectively. Then the adaptive finite-time fuzzy control scheme was proposed. In Ref. [15], fuzzy logic control was designed by combining PID control to reduce the vibration. The comparison simulation verified its good performance. Shalabi et al [16] utilized the Neuro-fuzzy inference system to air suspension system and guaranteed ride comfort and handling stability by controlling solenoid valves. An experiment was carried out to verify the effectiveness of the controller. In Ref. [17], [18], the sliding mode control was integrated with FLS to enhance ride comfort. Specifically, the NNs and FLS were combined in Ref. [17]. Both NNs and FLS are powerful tools to deal with the unknown nonlinearity and uncertainty. However, with the increase in the number of neurons in NNs, the computational burden increases, although the approximation error gets smaller. This is also observed with the FLS. The approximating results become precise with the increase in logic rules, but the calculation becomes complicated.

Bechlioulis et al. [19] first proposed the prescribed performance control (PPC) to simplify the design procedure and relieve the calculation burden. The main idea of PPC is to preset a performance function that defines the controlled plant's convergence rate, overshoot range and signal convergence boundary. Thus, it can ensure both transient and steady state performance of systems. Then they extended the method to the MIMO system [20] and combined it with the partial state feedback method for an unknown nonlinear system [21]. Moreover, its structure was further simplified [22], similar to the recursion scheme of backstepping control but avoided the problem of 'explosion of complexity' existing in backstepping. Subsequently, this method was applied to nonlinear suspension systems [23]–[25] and some other systems [21], [26]–[29] like servo mechanisms and MEMS gyroscopes and obtained considerable results. Unlike the control scheme using approximation function, such as NNs and FLS, the PPC does not require any other control methods' assistance to complete the control goal, and its simple scheme reduces computation time meanwhile. However, the simple structure also results in its sensibility to rapidly changing signals and limits the ability of PPC to suppress vibration for suspensions. Thus, there is a need to find an auxiliary method to enhance its vibration suppression performance. Although the performance of active suspension systems is improved a lot by applying various control methods like that mentioned above, vibration suppressing is still an important issue to be further enhanced due to the complex dynamic structure and changeable working environment. Pan et al [30] first used the bioinspired structure as a reference model in a nonlinear suspension system

to isolate more vibration, while this structure was initially regarded as a vibration isolator in Ref. [31]. Subsequently, various control methods such as fuzzy adaptive control, fuzzy sliding mode control and adaptive neural network control were implemented to enhance the performance of the suspension system with the bioinspired reference model [32]–[34], considering uncertainty and unknown nonlinearity. The main merit of introducing the bioinspired model is to utilize the beneficial nonlinearity inside, which is useful to suppress vibration of the system. However, it should be noted that the fuzzy method and neural networks were the primary tools to deal with uncertainty and unknown nonlinearity in these works. Their common defects of complex structure and computing redundancy as mentioned before remain still. Therefore, this paper proposes the approximation-free control based on the bioinspired reference model for the suspension system with uncertainty and unknown nonlinearity.

The primary contributions of this paper are concluded as follows: Firstly, compared to controllers with the FLS or NNs approximators in [32]–[34], the proposed control scheme is a simple structure that has a similar but more concise recursive framework of backstepping control and possesses the merit to handle inexact model without approximation. The simple structure releases the calculation burden and saves significant time. Furthermore, the acceleration decreases due to the bioinspired reference model and PPF, resulting in improved comfort but guaranteed road-handling. Secondly, due to the prescribed performance function in the proposed controller, the tracking error can be converged sooner and the ultimate convergence bound can be remained in a smaller region than the comparison subject (fuzzy adaptive control (FAC) [32]). Then it enhances the system convergence performance and helps the active suspension system respond quickly and precisely in reality. In particular, for the first time in this paper, the superior convergence performance of PPF is theoretically compared to FLS. This helps in the practical design of the controller.

The rest of this paper is organized as follows. In Section 2, the suspension system model and the bioinspired model are formed and some prior conditions are presented. The scheme of approximation-free control based on the bioinspired reference model is established and the stability proof and convergence performance analysis are given in Section 3. Then, the validity and superiority are verified by simulation and comparison in Section 4. Finally, the conclusion is presented in Section 5.

II. PROBLEM FORMULATION

The whole structure of the suspension system tracking the bioinspired model under the approximation-free control can be described in Fig 1. For the part of the active suspension system in Fig 1, we can get the following dynamic equations of the suspension system based on Newton's second law.

$$\begin{aligned} m_s \ddot{z}_s + F_d(\dot{z}_s, \dot{z}_u) + F_s(z_s, z_u) &= u \\ m_u \ddot{z}_u - F_d(\dot{z}_s, \dot{z}_u) - F_s(z_s, z_u) + F_t(z_u, z_r) &+ \\ F_b(\dot{z}_u, \dot{z}_r) &= -u \end{aligned} \quad (1)$$

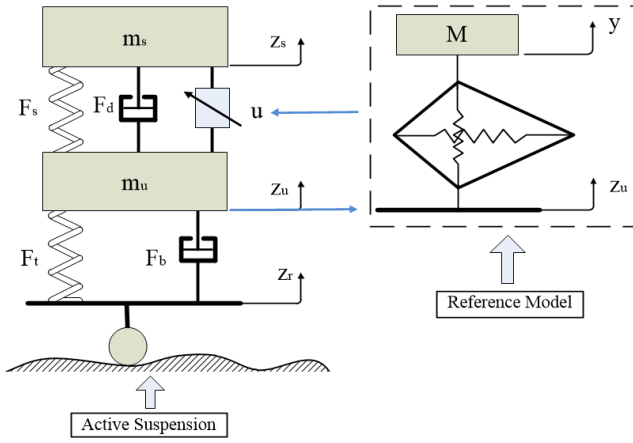


Fig. 1. Whole structure of suspension system with the bioinspired reference model.

where

$$\begin{aligned} F_t &= k_t(z_u - z_r) \\ F_b &= c_t(\dot{z}_u - \dot{z}_r) \end{aligned}$$

m_s represents sprung mass, which is an uncertain term owing to the change in passengers; m_u is the unsprung mass; z_s and z_u are absolute displacements of sprung mass, unsprung mass respected to ground, respectively; z_r denotes the road excitation; u is the input force from the designed controller; F_s and F_d are unknown nonlinear forces produced by springs and dampers, respectively; Elastic and damping forces of tire are denoted by F_t and F_b , respectively; For the convenience of subsequent analysis, some assumptions for the suspension system should be given here.

Assumption 1 The uncertain term in (1) is bounded and assumed to satisfy that $m_s \in \Omega_{m_s} = \{m_s : m_{s \min} \leq m_s \leq m_{s \max}\}$, where $m_{s \min}$ and $m_{s \max}$ are lower and upper bound of sprung mass, respectively.

Assumption 2 The unknown nonlinear forces F_s and F_d are bounded and continuous, which is described by inequalities: $|F_s| < \bar{F}_s$ and $|F_d| < \bar{F}_d$.

Assumption 3 The road excitation z_r and corresponding derivative \dot{z}_r are limited, Given the positive constant \bar{z}_{r1} and \bar{z}_{r2} , they are satisfied that $|z_r| < \bar{z}_{r1}$ and $|\dot{z}_r| < \bar{z}_{r2}$.

We can further rewrite (1) to state-space form. Defining state vector $[x_1, x_2, x_3, x_4] = [z_s, \dot{z}_s, z_u, \dot{z}_u]$, state-space equation can be represented as

$$\begin{cases} \dot{x}_1 = x_2 \\ \dot{x}_2 = \frac{1}{m_s}(-F_d(x_2, x_4) - F_s(x_1, x_3) + u) \\ \dot{x}_3 = x_4 \\ \dot{x}_4 = \frac{1}{m_u}(F_d(x_2, x_4) + F_s(x_1, x_3) - F_t(x_3, z_r) - F_b(x_4, \dot{z}_r) - u) \end{cases} \quad (2)$$

Besides, by defining the relative displacement as state, that is, state vector $[z_1, z_2] = [z_s - z_u, \dot{z}_s - \dot{z}_u]$, one can obtain the relative state-space form inferred from (1)

$$\begin{cases} \dot{z}_1 = z_2 \\ \dot{z}_2 = \ddot{z}_s - \ddot{z}_u = \theta(\chi(z_1, z_2) + u) - \ddot{z}_u \end{cases} \quad (3)$$

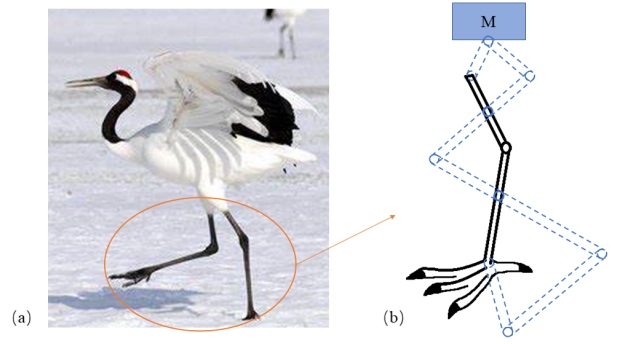


Fig. 2. Dynamic structure of Grus Japonensis's leg [31].

where the coefficient $\theta = 1/m_s$, and nonlinear term $\chi = -F_s - F_d$. Furthermore, the suspension system should satisfy the following constraints to ensure safety. One is that the dynamic load of the tire during driving is less than the weight of the vehicle so that the tire can keep uninterrupted contact with the road. Another one is that the suspension dynamic deflection in riding can not exceed the max suspension stroke. The following equations express the relationship

$$F_t + F_b < (m_s + m_u)g \quad (4)$$

$$z_s - z_u < z_{\max} \quad (5)$$

Next, the bioinspired model to be used in control design is discussed. Grus Japonensis's leg inspires the part of the bioinspired reference model in Fig 1. The Japonensis's leg structure is displayed in Fig 2 (a), and the corresponding equivalent dynamic structure is depicted in Fig 2 (b). For a more detailed analysis of bioinspired structure, one can refer to [31].

The bioinspired structure can be further simplified into an X-shape structure, shown in Fig 3 (a), consisting of two shorter rods, two longer rods, one vertical spring, and one horizontal spring. The motion during extension is described in Fig 3 (b). The force condition of different joints is depicted in Fig 3 (c). M is the mass of vibration isolated target. x and y express the absolute horizontal displacement of joints 1 and 3 and the absolute vertical displacement of M , respectively. x_1 and x_2 are the relative displacement of joint 1 and joint 3 with respect to the original position, respectively. y_r represents the relative displacement of joints 1 and 3 in compression or extension respected to that in the initial position. L_1 and L_2 are the length of the rod, which satisfy $L_1 < L_2$. θ_1 and θ_2 are angles between rod and base, which meet $\theta_1 > \theta_2$. φ_1 and φ_2 are relative angles respected to initial angle when rod rotates. k_h and k_v represent the stiffness coefficient of horizontal and vertical spring in the model, respectively. z_u is the road excitation.

The dynamic analysis of the bioinspired model is given in Appendix I. The nonlinear dynamic equation can be written as follows by defining $y_r = y - z_u$.

$$M\ddot{y}_r + h_1(y_r) + k_v y_r + \mu_1 \dot{y}_r + \mu_2 n_x h_2(y_r) \dot{y}_r = -M\ddot{z}_u \quad (6)$$

where μ_1 and μ_2 are the air damping coefficient and rotational friction coefficient, respectively. n_x is the number of

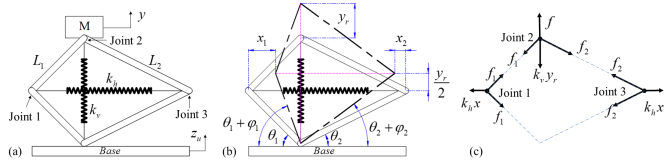


Fig. 3. Geometry structure of the bioinspired model and dynamic analysis.

joints. $h_1(y_r)$ and $h_2(y_r)$ can be expressed (7) by defining $y_1 = y_r$, $y_2 = \dot{y}_r$, $v(y_1) = L_1 \sin \theta_1 + y_1/2$, and $\sigma_i = \sqrt{L_i^2 - v^2(y_1)}$ ($i = 1, 2$). Then defining $f(y_1) = h_1(y_1) + k_v y_1$, and $g(y_1, y_2) = \mu_1 y_2 + \mu_2 n_x h_2(y_1) y_2$, the state-space form of the bioinspired model is obtained, shown in (8).

$$\begin{cases} h_1(y_1) = \frac{k_h}{2} (L_1 \cos \theta_1 + L_2 \cos \theta_2 - \sigma_1 - \sigma_2) \\ \quad \cdot (v(y_1)/\sigma_1 + v(y_1)/\sigma_2) \\ h_2(y_1) = (1/(2\sigma_1) + 1/(2\sigma_2)) \end{cases} \quad (7)$$

$$\begin{cases} \dot{y}_1 = y_2 \\ \dot{y}_2 = -\frac{1}{M} (f(y_1) + g(y_1, y_2)) - \ddot{z}_u \end{cases} \quad (8)$$

Equation (8) represents the relationship of internal parameter and dynamic behavior of the bioinspired structure, which will be used as a reference model for the active suspension system in Fig 1. It is worth noting that the bioinspired structure containing nonlinearity is beneficial for vibration suppression when designing the controller [32].

It is necessary to investigate the stability of the bioinspired model to facilitate subsequent analysis. The conclusion of stability analysis will be given first here.

Lemma1 [32]: Define state vector as $\bar{y} = [y_1, y_2]$ ($|y_1| < \min(L_1 \sin \theta_1, L_1(1 - \sin \theta_1)), y_2 \in R$). Assume that the disturbance is bounded and satisfies $|\ddot{z}_u| < \delta \leq \zeta \|\bar{y}\|_2 / \sqrt{(\mu_1/M)^2 + 4}$ for all $t \geq 0$, where $\zeta = \min\{(\mu_1/M^2)k_v, (1/M)(\mu_1/M + 2\mu_2 n_x \vartheta)\}$ and $\vartheta = (L_1 + L_2)/(2L_1 L_2)$, then the bioinspired system (8) will uniformly ultimately bounded.

III. APPROXIMATION-FREE CONTROLLER DESIGN AND ANALYSIS

Before designing the controller, it is necessary to introduce some definitions and theorems, which will be used in subsequent analysis. Given the differential equation and its initial value:

$$\dot{\eta}(t) = f(t, \eta(t)), \eta(0) = \eta^0 \in \Omega_\eta. \quad (9)$$

where $f: \mathbb{R}_+ \times \Omega_\xi \rightarrow \mathbb{R}^n$, and $\Omega_\xi \subset \mathbb{R}^n$ is a non-empty open set.

Definition1 [35] A solution of the initial value problem (9) (i.e., $t \mapsto \eta(t)$) is maximal if it has no proper right extension, and it is also a solution for the problem (9).

Lemma2 [35] Consider the initial value problem (9). Assume that f is: (a) locally Lipschitz on η , (b) continuous on t for each fixed $\eta \in \Omega_\eta$ and (c) locally integrable on t

for each fixed $\eta \in \Omega_\eta$. Then, a unique maximal solution exists $\eta: [0, \tau_{\max}) \rightarrow \Omega_\eta$ of (9) on the time interval $[0, \tau_{\max})$ with $\tau_{\max} \in \{\mathbb{R}_+^*, \infty\}$ such that $\eta(t) \in \Omega_\eta, \forall t \in [0, \tau_{\max})$.

Proposition1 [35] Assume that the hypotheses of Lemma 2 hold. For a maximal solution $\eta: [0, \tau_{\max}) \rightarrow \Omega_\eta$ on the time $[0, \tau_{\max})$ with $\tau_{\max} < \infty$ and for any compact set $\Omega'_\eta \subset \Omega_\eta$, there exists a time instant $t' \in [0, \tau_{\max})$ such that $\eta(t') \notin \Omega'_\eta$.

A. Prescribed performance function

The tracking error will be transformed to an equivalent error described by a prescribed performance function (PPF). The PPF is a smooth function designed to presuppose the needed performance parameters such as overshoot, the convergence rate, and the ultimate convergence bound of system tracking error. The PPF has the following characteristics: $\rho: \mathbb{R}^+ \rightarrow \mathbb{R}^+$, and its value decreases with time. Furthermore, $\lim_{t \rightarrow \infty} \rho(t) = \rho_\infty > 0$, where ρ_∞ is a known constant. Then, the expression $\rho(t) = (\rho_0 - \rho_\infty)e^{-lt} + \rho_\infty$ ($\rho_0 > \rho_\infty > 0$) can be one of the possible functions.

Given the upper bound δ_U and lower bound δ_L and assuming that the tracking error of the system is presented by $e(t)$, then it can be confined to an arbitrarily small set defined by PPF after being controlled, that is

$$-\delta_L \rho(t) < e(t) < \delta_U \rho(t) \quad (10)$$

In order to transform the constraint condition in (10) to unconstrained one, another function $S(\varepsilon)$ is needed, which has the following properties. (1) $S(\varepsilon)$ is smooth; (2) $-\delta_L < S(\varepsilon) < \delta_U$, $\varepsilon \in (-\infty, +\infty)$; (3) $\lim_{\varepsilon \rightarrow -\infty} S(\varepsilon) = -\delta_L$, $\lim_{\varepsilon \rightarrow +\infty} S(\varepsilon) = \delta_U$. The function can be chosen as

$$S(\varepsilon) = \frac{\delta_U e^\varepsilon - \delta_L e^{-\varepsilon}}{e^\varepsilon + e^{-\varepsilon}} \quad (11)$$

where δ_U and δ_L are positive constant. Then, making $S(\varepsilon) = e(t)/\rho(t)$ and combining (10) and (11), one has that

$$\varepsilon = S^{-1}(\xi) = \ln \left(\frac{\delta_L + \xi}{\delta_U - \xi} \right) \quad (12)$$

where $\xi = e(t)/\rho(t)$. Hence, the original error $e(t)$ is transformed to equivalent error ε , which varies from minus infinity to infinity. Hence, the control problem can be solved by guaranteeing transformed error ε bound; then it ensures the error $e(t)$ in (10) can be controlled to a compact set if the parameters l , ρ_∞ , ρ_0 , δ_L , and δ_U are chosen properly.

Remark1 The prescribed performance function $\rho(t)$ can be designed as asymmetric form based on situations; that is, the prescribed function can consist of upper bound function $\rho(t)_U$ and lower bound function $\rho(t)_L$, then ξ is described by the following function:

$$\xi = \frac{e(t) - \frac{\rho(t)_U - \rho(t)_L}{2}}{\frac{\rho(t)_U + \rho(t)_L}{2}}$$

B. Proposed theorem and proof

Considering the absolute state-space equation (2) and the relative state-space equation (3) of the suspension system that tracks the bioinspired reference model (8), the approximation-free controller can be designed in three steps. The design procedures are similar to those of backstepping control recursion framework.

Step1 : Define the relative displacement error in (13) and the intermediate virtual control function as follows:

$$e_1(t) = z_1(t) - y_1(t) \quad (13)$$

$$u_1 = -k_1 \varepsilon_1 = -k_1 \ln \left(\frac{\delta_{L1} + \xi_1}{\delta_{U1} - \xi_1} \right) \quad (14)$$

where k_1 is positive control gain; δ_{L1} , and δ_{U1} are positive, and their values are defined by users. ξ_1 satisfies that $\xi_1(t) = e_1(t)/\rho_1(t)$. $\rho_1(t)$ is prescribed performance function, i.e., $\rho_1(t) = (\rho_{10} - \rho_{1\infty}) e^{-l_1 t} + \rho_{1\infty}$, where ρ_{10} is the initial value and satisfies $\min \{\delta_{L1}, \delta_{U1}\} \rho_{10} > |e_1(0)| = |z_1(0) - y_1(0)|$, $\rho_{1\infty}$ is the boundary to make relative displacement error converges to a compact set and l_1 represents the convergence rate. Users also define their values.

Step2 : Based on the first intermediate virtual control u_1 defined in Step 1, the error of relative velocity is given in (15). The second intermediate virtual control u_2 can be designed as (16) shown

$$e_2(t) = z_2(t) - y_2(t) - u_1 \quad (15)$$

$$u_2 = -\frac{1}{\theta} k_2 \varepsilon_2 = -\frac{1}{\theta} k_2 \ln \left(\frac{\delta_{L2} + \xi_2}{\delta_{U2} - \xi_2} \right) \quad (16)$$

where k_2 , δ_{L2} and δ_{U2} are all positive, and their values are user-defined. Moreover $\xi_2(t) = e_2(t)/\rho_2(t)$, where $\rho_2(t) = (\rho_{20} - \rho_{2\infty}) e^{-l_2 t} + \rho_{2\infty}$. ρ_{20} , $\rho_{2\infty}$ and l_2 have similar definitions in Step 1. Also, ρ_{20} needs to satisfy that $\min \{\delta_{L2}, \delta_{U2}\} \rho_{20} > |e_2(0)| = |z_2(0) - y_2(0) - u_1(0)|$.

Step3 : Repeating the same procedure as Step 2, one can define the following absolute velocity error and final controller by virtue of the second virtual control u_2

$$e_3(t) = x_2(t) - u_2 \quad (17)$$

$$u = -\frac{1}{\theta} k_3 \varepsilon_3 = -\frac{1}{\theta} k_3 \ln \left(\frac{\delta_{L3} + \xi_3}{\delta_{U3} - \xi_3} \right) \quad (18)$$

where $\xi_3(t) = e_3(t)/\rho_3(t)$, $\rho_3(t) = (\rho_{30} - \rho_{3\infty}) e^{-l_3 t} + \rho_{3\infty}$ and $\min \{\delta_{L3}, \delta_{U3}\} \rho_{30} > |e_3(0)| = |x_2(0) - u_2(0)|$. Also, ρ_{30} , $\rho_{3\infty}$, l_3 , k_3 , δ_{L3} and δ_{U3} have similar definition and features as ρ_{i0} , $\rho_{i\infty}$, l_i , k_i , δ_{Li} and δ_{Ui} ($i = 1, 2$) in Step 1 and Step 2. Additionally, u should satisfy $|u| > |u_1 + u_2|$. Based on the definition of $\rho_i(t)$, $i = 1, 2, 3$, one can infer that $-\delta_{Li} < \xi_i(t) = e_i(t)/\rho_i(t) < \delta_{Ui}$, $i = 1, 2, 3$.

Remark2 : Though the approximation-free control based on the bioinspired model has a similar recursion design procedure as backstepping control, the scheme is simpler than backstepping control requiring the adaptive law and the derivative of intermedial virtual control in [30], which can be seen from aforementioned. Besides, the simple control scheme

avoids the requirement for the knowledge of nonlinearity. Furthermore, the approximators such as FLS or NNs are avoided here compared to [32]–[34], which reduces the computation complexity.

Remark3 : The suspension system's absolute velocity error is considered in the control design in Step 3. It is known that the acceleration of the vehicle plays a vital role in riding comfort for human beings. However, the tracking trajectory is dominated by relative states, which means that the design of first and second virtual control only assures convergence of the closed-loop system's relative signal. It is necessary to consider the absolute state in the design to confine the absolute acceleration simultaneously, and the final velocity state is a good choice which is the link between absolute displacement state and acceleration one. That is the main aim of Step 3.

Theorem 1 concludes the discussion above.

Theorem1 : Consider the absolute state-space equation (2) and relative one (3) of the suspension system. Assuming the initial state value $\min \{\delta_{Li}, \delta_{Ui}\} \rho_{i0} > |e_i(0)|$, $i = 1, 2, 3$ fulfilled and given the bioinspired reference model (8), the transformed error ε_i , $i = 1, 2, 3$ is guaranteed to be bounded under the control scheme (13)-(18) with the condition $|u| > |u_1 + u_2|$, which retains within the range $-\delta_{Li} < \xi_i < \delta_{Ui}$, $i = 1, 2, 3$, so that the tracking error and acceleration of suspension will converge to a small residual set by the assistant of PPF.

Proof : With the knowledge that $e_i(t)/\rho_i(t)$, $i = 1, 2, 3$ and considering the expressions (13)-(18), the state variables in (3) can be presented as $z_1 = \xi_1 \rho_1 + y_1$ and $z_2 = \xi_2 \rho_2 + y_2 + u_1$. Then, the derivative of $\xi_i(t)$, $i = 1, 2, 3$ with respect to time can be deduced as follows:

$$\begin{aligned} \dot{\xi}_1 &= (\dot{e}_1 \rho_1 - e_1 \dot{\rho}_1) / \rho_1^2 = ((\dot{z}_1 - \dot{y}_1) - \xi_1 \dot{\rho}_1) / \rho_1 \\ &= (\xi_2 \rho_2 + u_1 (\xi_1) - \xi_1 \dot{\rho}_1) / \rho_1 = \psi_1(t, \xi_1, \xi_2) \end{aligned} \quad (19)$$

$$\begin{aligned} \dot{\xi}_2 &= (\dot{e}_2 \rho_2 - e_2 \dot{\rho}_2) / \rho_2^2 = ((\dot{z}_2 - \dot{y}_2 - \dot{u}_1) - \xi_2 \dot{\rho}_2) / \rho_2 \\ &= ((\dot{z}_2 - \dot{y}_2 - \dot{u}_1) - \xi_2 \dot{\rho}_2) / \rho_2 \\ &= (\theta \chi (\xi_1 \rho_1 + y_1, \xi_2 \rho_2 + y_2 + u_1) + \theta u (\xi_3) \\ &\quad + \frac{1}{M} (f(y_1) + g(y_1, y_2)) - \dot{u}_1 - \xi_2 \dot{\rho}_2) / \rho_2 \end{aligned} \quad (20)$$

$$\begin{aligned} \dot{\xi}_3 &= (\dot{e}_3 \rho_3 - e_3 \dot{\rho}_3) / \rho_3^2 = ((\dot{x}_2 - \dot{u}_2) - \xi_3 \dot{\rho}_3) / \rho_3 \\ &= (\theta \chi (\xi_1 \rho_1 + y_1, \xi_2 \rho_2 + y_2 + u_1) + \theta u (\xi_3) \\ &\quad - \dot{u}_2 - \xi_3 \dot{\rho}_3) / \rho_3 \\ &= \psi_3(t, \xi_1, \xi_2, \xi_3) \end{aligned} \quad (21)$$

(19)-(21) can be further expressed by

$$\dot{\xi} = \psi(t, \xi) = \begin{bmatrix} \psi_1(t, \xi_1, \xi_2) \\ \psi_2(t, \xi_1, \xi_2, \xi_3) \\ \psi_3(t, \xi_1, \xi_2, \xi_3) \end{bmatrix} \quad (22)$$

There are two phases to complete the proof. The first phase ensures the existence and uniqueness of a maximal solution $\xi : [0, \tau_{\max}) \rightarrow \Omega_\xi$ of (22), where $\Omega_\xi = (-\delta_{L1}, \delta_{U1}) \times (-\delta_{L2}, \delta_{U2}) \times (-\delta_{L3}, \delta_{U3})$. Secondly, the transformed errors ε_i , $i = 1, 2, 3$ need to be bounded under the proposed controller over the time interval $t \in (0, \tau_{\max})$, which ensures the

system stability. Subsequently, the theorem is extended to the global one by proving $\tau_{\max} = +\infty$.

PhaseA With the condition $\min\{\delta_{Li}, \delta_{Ui}\} \rho_{i0} > |e_i(0)|$, $i = 1, 2, 3$, it's clear that the initial value of ξ satisfies $|\xi_i(0)| < \min\{\delta_{Li}, \delta_{Ui}\}$, $i = 1, 2, 3$, i.e., $\xi(0) \in \Omega_\xi$. Besides, the state vector $[y_1, y_2]$ of bioinspired reference model has already been proved bounded in Section 2. Furthermore, the suspension system and prescribed performance function ρ_i , $i = 1, 2, 3$ are continuous and differentiable. Then $\psi(t, \xi)$ in (22) is continuous and differentiable and satisfies the locally Lipschitz condition, which implies Lemma 2 can be applied here. Hence, there exists a maximal solution $\xi : [0, \tau_{\max}) \rightarrow \Omega_\xi$ such that $\xi(t) \in \Omega_\xi, \forall t \in [0, \tau_{\max})$, that is, $|\xi_i(t)| < \min\{\delta_{Li}, \delta_{Ui}\}$, $i = 1, 2, 3, \forall t \in [0, \tau_{\max})$.

PhaseB Based on the definition of the prescribed performance function and the characteristic of the designed controller, we know that system's stability is guaranteed if the transformed error ε_i , $i = 1, 2, 3$ remains bounded. For transformed error $\varepsilon_1 = \ln((\delta_{L1} + \xi_1)/(\delta_{U1} - \xi_1))$, the following Lyapunov function (23) is constructed.

$$V_1 = \frac{1}{2}\varepsilon_1^2 \quad (23)$$

Taking the derivative of equation (23) for $t \in [0, \tau_{\max})$, and substituting equation (19), one has that

$$\begin{aligned} \dot{V}_1 &= \varepsilon_1 \dot{\varepsilon}_1 \\ &= \varepsilon_1 \left(\frac{\delta_{U1} + \delta_{L1}}{(\delta_{L1} + \xi_1)(\delta_{U1} - \xi_1)} \dot{\xi}_1 \right) \\ &= \frac{\delta_{U1} + \delta_{L1}}{(\delta_{L1} + \xi_1)(\delta_{U1} - \xi_1)\rho_1} \varepsilon_1 (\dot{z}_1 - \dot{y}_1 - \xi_1 \dot{\rho}_1) \end{aligned} \quad (24)$$

Making $r_1 = (\delta_{U1} + \delta_{L1})/((\delta_{L1} + \xi_1)(\delta_{U1} - \xi_1)\rho_1)$. With the knowledge that δ_{U1} , and δ_{L1} are positive and bounded, ρ_1 , and ρ_2 are positive continuous bounded functions, and ξ_1 satisfies $-\delta_{L1} < \xi_1 < \delta_{U1}$, then it can be inferred that $r_1 > 0$. Taking account into $\dot{z}_1 - \dot{y}_1 = z_2 - y_2 = e_2 + u_1$, it follows from (24) that

$$\begin{aligned} \dot{V}_1 &= r_1 \varepsilon_1 (e_2 + u_1 - \xi_1 \dot{\rho}_1) = r_1 \varepsilon_1 (\xi_2 \rho_2 - k_1 \varepsilon_1 - \xi_1 \dot{\rho}_1) \\ &\leq r_1 \left(|\varepsilon_1| \bar{Q}_1 - k_1 |\varepsilon_1|^2 \right) \end{aligned} \quad (25)$$

where \bar{Q}_1 is a positive constant representing bound of $|\xi_2 \rho_2 - \xi_1 \dot{\rho}_1|$. We know that ρ_1 is continuous and monotonically decreasing, thus $\dot{\rho}_1$ is bounded. Besides, ξ_2 is bounded and satisfies that $-\delta_{L2} < \xi_2 < \delta_{U2}$. Therefore, the conclusion is that $|\xi_2 \rho_2 - \xi_1 \dot{\rho}_1|$ is bounded based on the Extreme Value Theorem, then it is represented by the supremum \bar{Q}_1 , i.e., $\bar{Q}_1 = \sup\{|\xi_2 \rho_2 - \xi_1 \dot{\rho}_1|\}$. Hence, \dot{V}_1 is negative if ε_1 satisfies the condition $|\varepsilon_1| > \bar{Q}_1/k_1$. Consequently, we have the conclusion that the transformed error ε_1 will converge to compact set $\Omega_1 = \{\varepsilon_1 \mid |\varepsilon_1| < \bar{\varepsilon}_1\}$ with $\bar{\varepsilon}_1 = \max\{|\varepsilon_1(0)|, \bar{Q}_1/k_1\}$, $\forall t \in [0, \tau_{\max})$, based on Lyapunov Theorem. In addition, the first intermediate virtual control $u_1 = -k_1 \varepsilon_1$ is bounded.

Next, the similar Lyapunov function is given to prove the second transformed error $\varepsilon_2 = \ln((\delta_{L2} + \xi_2)/(\delta_{U2} - \xi_2))$ as

follows:

$$V_2 = \frac{1}{2}\varepsilon_2^2 \quad (26)$$

Then for $t \in [0, \tau_{\max})$ the following derivative of (26) can be obtained by substituting (20), (3) and (8)

$$\begin{aligned} \dot{V}_2 &= \varepsilon_2 \dot{\varepsilon}_2 \\ &= \varepsilon_2 \left(\frac{\delta_{U2} + \delta_{L2}}{(\delta_{L2} + \xi_2)(\delta_{U2} - \xi_2)} \dot{\xi}_2 \right) \\ &= \frac{\delta_{U2} + \delta_{L2}}{(\delta_{L2} + \xi_2)(\delta_{U2} - \xi_2)\rho_2} \varepsilon_2 (\dot{z}_2 - \dot{y}_2 - \dot{u}_1 - \xi_2 \dot{\rho}_2) \\ &= r_2 \varepsilon_2 (\theta \chi(z_1, z_2) + \theta u + (1/M)(f(y_1) + g(y_1, y_2)) \\ &\quad - \dot{u}_1 - \xi_2 \dot{\rho}_2) \end{aligned} \quad (27)$$

where $r_2 = (\delta_{U2} + \delta_{L2})/((\delta_{L2} + \xi_2)(\delta_{U2} - \xi_2)\rho_2)$. With the condition that δ_{U2} , and δ_{L2} are positive and satisfies that $-\delta_{L2} < \xi_2 < \delta_{U2}$, then $(\delta_{L2} + \xi_2)(\delta_{U2} - \xi_2) > 0$. Besides, ρ_2 is positive. Therefore, it is deduced that r_2 is positive. Assuming that $|u| > |u_1 + u_2|$ and introducing the condition $z_1 = \xi_1 \rho_1 + y_1$ and $z_2 = \xi_2 \rho_2 + y_2 + u_1$, it can be further derived from (27) that

$$\begin{aligned} \dot{V}_2 &\leq r_2 \varepsilon_2 (\theta \chi(\xi_1 \rho_1 + y_1, \xi_2 \rho_2 + y_2 + u_1) + \theta(u_1 + u_2)) \\ &\quad + \frac{1}{M}(f(y_1) + g(y_1, y_2)) - \dot{u}_1 - \xi_2 \dot{\rho}_2 \\ &= r_2 \varepsilon_2 (\theta \chi(\xi_1 \rho_1 + y_1, \xi_2 \rho_2 + y_2 + u_1) + \theta u_1 - k_2 \varepsilon_2) \\ &\quad + \frac{1}{M}(f(y_1) + g(y_1, y_2)) - \dot{u}_1 - \xi_2 \dot{\rho}_2 \\ &\leq r_2 \left(|\varepsilon_2| \bar{Q}_2 - k_2 |\varepsilon_2|^2 \right) \end{aligned} \quad (28)$$

where $\bar{Q}_2 = \sup\{|\theta \chi + \theta u_1 + (1/M)/(f + g) - \dot{u}_1 - \xi_2 \dot{\rho}_2|\}$. For simplicity, $\chi(\xi_1 \rho_1 + y_1, \xi_2 \rho_2 + y_2 + u_1)$, $f(y_1)$, and $g(y_1, y_2)$ in (28) are abbreviated by χ , f , and g , respectively. According to lemma 1, the bioinspired model (8) is uniformly ultimately bounded, which means y_1, y_2 and $(1/M)/(f + g)$ are bounded. With the assumption that F_s and F_d are continuous and bound, we know that $\chi = -F_d - F_s$ is bounded. Besides, u_1 and ρ_2 are bounded and continuous, which indicates that \dot{u}_1 , and $\dot{\rho}_2$ are also bounded. Consequently, applying the Extreme Value Theorem, $|\theta \chi + \theta u_1 + (1/M)/(f + g) - \dot{u}_1 - \xi_2 \dot{\rho}_2|$ has an upper bound, denoted by \bar{Q}_2 . As a consequence, \dot{V}_2 is negative if $|\varepsilon_2| > \bar{Q}_2/k_2$ and according to Lyapunov Theorem, ε_2 will converge to compact set $\Omega_2 = \{\varepsilon_2 \mid |\varepsilon_2| < \bar{\varepsilon}_2\}$ with $\bar{\varepsilon}_2 = \max\{|\varepsilon_2(0)|, \bar{Q}_2/k_2\}$, $\forall t \in [0, \tau_{\max})$. Then, the second intermediate virtual control $u_2 = -k_2 \varepsilon_2$ is also guaranteed to be bounded.

Remark4 The reason for using the condition $|u| > |u_1 + u_2|$ is presented here. It is easy to know that $\varepsilon_i, i = 1, 2, 3$ have opposite sign against $u_i, i = 1, 2, 3 (u = u_3)$ according to their expressions. As mentioned above, one has that $\varepsilon_3 = \ln((\delta_{L3} + \xi_3)/(\delta_{U3} - \xi_3))$ and $\xi_3 = (x_2 + k_2 \varepsilon_2)/\rho_3$. The partial differential of ε_3 with respect to ξ_3 and the partial differential of ξ_3 with respect to ε_2 is positive according to $k_2 > 0, \rho_3 > 0$, and $(\delta_{U2} + \delta_{L2})/((\delta_{L2} + \xi_2)(\delta_{U2} - \xi_2)) > 0$. Besides, if $\varepsilon_2 \rightarrow 0$, then $\xi_3 \rightarrow 0$ is satisfied due to the

expressions of ε_2 and ξ_3 . Also, if $\xi_3 \rightarrow 0$ then $\varepsilon_3 \rightarrow 0$ is required based on the control goal. Therefore, ε_2 has the same sign as ε_3 and u has a sign opposite of ε_2 . By analogy, one can conclude that $\varepsilon_i, i = 1, 2, 3$ and $u_i, i = 1, 2, 3 (u = u_3)$ have the same sign with each other, respectively, but $\varepsilon_i, i = 1, 2, 3$ have opposite sign against $u_i, i = 1, 2, 3 (u = u_3)$, which helps the use of the condition $|u| > |u_1 + u_2|$ in (28).

In the same manner, the similar Lyapunov structure is presented for the third transformed error $\varepsilon_3 = \ln((\delta_{L3} + \xi_3)/(\delta_{U3} - \xi_3))$

$$V_3 = \frac{1}{2} \varepsilon_3^2 \quad (29)$$

Introducing (21), the derivative of (29) can be deduced as follows:

$$\begin{aligned} \dot{V}_3 &= \varepsilon_3 \dot{\varepsilon}_3 \\ &= \varepsilon_3 \left(\frac{\delta_{U3} + \delta_{L3}}{(\delta_{L3} + \xi_3)(\delta_{U3} - \xi_3)} \dot{\xi}_3 \right) \\ &= \frac{\delta_{U3} + \delta_{L3}}{(\delta_{L3} + \xi_3)(\delta_{U3} - \xi_3) \rho_3} \varepsilon_3 (\dot{x}_2 - \dot{u}_2 - \xi_3 \dot{\rho}_3) \end{aligned} \quad (30)$$

If $r_3 = (\delta_{U3} + \delta_{L3})/((\delta_{L3} + \xi_3)(\delta_{U3} - \xi_3) \rho_3)$ then $r_3 > 0$ as $-\delta_{L3} < \xi_3 < \delta_{U3}$, where δ_{U3} , δ_{L3} and ρ_3 are positive. Substituting absolute state-space form (2) of the suspension system, the expression (30) can be further derived into the following equation

$$\begin{aligned} \dot{V}_3 &= r_3 \varepsilon_3 (\theta(\chi(z_1, z_2) + u) - \dot{u}_2 - \xi_3 \dot{\rho}_3) \\ &= r_3 \varepsilon_3 (\theta(\chi(\xi_2 \rho_2 + y_2 + u_1, \xi_1 \rho_1 + y_1) - k_3 \varepsilon_3 \\ &\quad - \dot{u}_2 - \xi_3 \dot{\rho}_3) \\ &\leq r_3 (|\varepsilon_3| \bar{Q}_3 - k_3 |\varepsilon_3|^2) \end{aligned} \quad (31)$$

where $\bar{Q}_3 = \{|\theta(\chi(\xi_2 \rho_2 + y_2 + u_1, \xi_1 \rho_1 + y_1) - \dot{u}_2 - \xi_3 \dot{\rho}_3)|\}$. Because u_2 and ρ_3 are bounded and continuous, then \dot{u}_2 and $\dot{\rho}_3$ are all bounded. Consequently, according to the Extreme Value Theorem, there exists a supremum for $|\theta(\chi(\xi_2 \rho_2 + y_2 + u_1, \xi_1 \rho_1 + y_1) - \dot{u}_2 - \xi_3 \dot{\rho}_3)|$, which is represented by \bar{Q}_3

Therefore, \dot{V}_3 is negative for any $|\varepsilon_3| > \bar{Q}_3/k_3$. Then it is deduced from Lyapunov Theorem that ε_3 will converged to a compact set $\Omega_3 = \{\varepsilon_3 \mid |\varepsilon_3| < \bar{\varepsilon}_3\}$ with $\bar{\varepsilon}_3 = \max\{|\varepsilon_3(0)|, \bar{Q}_3/k_3\}, \forall t \in [0, \tau_{\max})$. Finally, it is concluded that the control force u is bounded. Consequently, the relative states z_1, z_2 and absolute state x_2 remain bounded. Moreover, one can obtain that

$$\begin{aligned} -\delta_{Li} &< \frac{e^{-\bar{\varepsilon}_i} \delta_{Ui} - \delta_{Li}}{e^{-\bar{\varepsilon}_i} + 1} = \xi_{Li} \leq \xi_i \\ \xi_i &\leq \xi_{Ui} = \frac{e^{\bar{\varepsilon}_i} \delta_{Ui} - \delta_{Li}}{e^{\bar{\varepsilon}_i} + 1} < \delta_{Ui}, i = 1, 2, 3, \forall t \in [0, \tau_{\max}) \end{aligned} \quad (32)$$

Defining the set $\Omega'_\xi = [\xi_{L1}, \xi_{U1}] \times [\xi_{L2}, \xi_{U2}] \times [\xi_{L3}, \xi_{U3}]$, it is obvious that $\Omega'_\xi < \Omega_\xi$ from (32). Assuming that $\tau_{\max} < +\infty$, we know that there exists a time instant $t' \in [0, \tau_{\max})$ such that $\xi_i(t') \notin \Omega'_\xi$ by applying Proposition 1, which is contradictory to what is expressed in (32). Thus, we have the conclusion that $\tau_{\max} = +\infty$ and Theorem 1 is applicable for $t \in [0, +\infty)$. The proof of Theorem 1 is complete.

C. Suspension ride safety analysis

Additionally, the suspension system needs to meet the requirements of ride safety mentioned in Section 2 and it will be analyzed next. From the above proof of Theorem 1, we know that relative displacement $z_1 = x_1 - x_3$ of sprung mass against unsprung mass can be confined to a reasonable residual set, that is, $-\delta_{L1} \rho_{10} < z_1 - y_1 < \delta_{U1} \rho_{10}$. It implies that the suspension deflection constraint (5) is guaranteed if parameters of controller δ_{L1} , δ_{U1} , and ρ_{10} are chosen appropriately, as well as parameters of bioinspired reference model. The bioinspired reference model (3) is a kind of vibration isolator and provide an ideal reference trajectory to controller. One can refer to Ref. [31] to choose appropriate parameters of bioinspired model. For dynamic tire load, the analysis is presented next. Considering state $[x_3, x_4]$, the following equation holds

$$\dot{x} = Ax + w \quad (33)$$

where

$$A = \begin{bmatrix} 0 & 1 \\ -\frac{k_t}{m_u} & -\frac{c_t}{m_u} \end{bmatrix}$$

and

$$w = \begin{bmatrix} 0 \\ \frac{1}{m_u} (-k_t z_r - c_t \dot{z}_r + F_d + F_s - u) \end{bmatrix}$$

Based on previous proof of theorem 1, it's known that u is bounded. Combining Assumption 2 and 3, it can be inferred that w has the limit, which is presented by $w \leq \bar{w}$. For the system (33), the Lyapunov function $V_x = x^T P x$ is constructed, where $P > 0$ is a symmetric matrix. Thus, its derivative can be obtained as $\dot{V}_x = x^T (A^T P + P A) x + 2w^T P x$. Moreover, the condition $A^T P + P A = -Q$ can be utilized since A is Hurwitz. Then Young's inequality can be applied in (33). Therefore, the derivative is further deduced by

$$\begin{aligned} \dot{V}_x &\leq -x^T Q x + \frac{\lambda_{\max}(P^2)}{\eta} \|x\|^2 + \eta \|w\|^2 \\ &\leq -(\lambda_{\min}(Q) - \lambda_{\max}(P^2)/\eta) \|x\|^2 + \eta \bar{w}^2 \\ &\leq -\ell V_x + W \end{aligned} \quad (34)$$

where $\ell = \lambda_{\min}(Q) - \lambda_{\max}(P^2)/\eta$, $W = \eta \bar{w}^2$ and η is a positive constant defined in Young's inequality. Integrating both sides of (34), one can obtain that

$$V_x(t) \leq V_x(0) e^{-\ell t} + W/\ell \leq V_x(0) + W/\ell \quad (35)$$

Therefore, from (35) it implies that suspension states x_3 and x_4 are bounded, that is, $|x_i| \leq \sqrt{(V_x(0) + W/\ell)/\lambda_{\min}(P)}, i = 3, 4$. Furthermore, based on Assumption 3, the following inequality holds

$$\begin{aligned} |F_t + F_b| &= |k_t(x_3 - z_r) + c_t(x_3 - \dot{z}_r)| \\ &\leq (k_t + c_t) \sqrt{(V_x(0) + W/\ell)/\lambda_{\min}(P)} \\ &\quad + k_t \bar{z}_{r1} + c_t \bar{z}_{r2} \end{aligned} \quad (36)$$

Consequently, the dynamic tyre load constraint (4) is guaranteed by designing appropriate parameters η and P that satisfy the inequality $(k_t + c_t) \cdot \sqrt{(V_x(0) + W/\ell)/\lambda_{\min}(P)} + k_t \bar{z}_{r1} + c_t \bar{z}_{r2} \leq (m_u + m_s)g$, which ensures ride holding performance of the suspension system.

D. Theoretical analysis in PPF superior convergence property

The property of preset transient performance of approximation-free controller makes it superior to the controller with FLS in convergence rate. In this part, the better convergence performance of the approximation-free controller will be analyzed theoretically.

Firstly, we will prove that the system controlled by FLS-controller with PPF converges faster than the one controlled by FLS-controller without PPF[29, 31], which confirms the effectiveness of transient property predefined by PPF. Before presenting the proof, the following inequality will be needed:

$$\left| \ln \left(\frac{a + \xi}{b - \xi} \right) \right| \geq \frac{4}{a + b} \left| \xi - \frac{b - a}{2} \right| \quad (37)$$

where $a > 0$, $b > 0$, and $-a < \xi < b$. The inequality (37) can be easily proved by dividing it into two parts: one for $\xi \in \{\xi | \xi > (b - a)/2\}$, another for $\xi \in \{\xi | \xi \leq (b - a)/2\}$, and taking the derivative.

Here the suspension system (3) tracking bioinspired model (8) is considered. Define the system state as $[x_{s1}, x_{s2}] = [z_1 - y_1, z_2 - y_2]$, error as $[e_1, e_2] = [x_{s1}, x_{s2} - \alpha_1]$, and intermediate virtual control as $\alpha_1 = -\lambda_1 e_1$, then the fuzzy control law and adaptive law can be designed as:

$$u = \frac{1}{\theta} (-\lambda_2 e_2 - e_1 - \hat{w}_1 \phi_1 + \dot{\alpha}_1) \quad (38)$$

$$\dot{\hat{w}}_1 = -e_2 \phi_1 \quad (39)$$

where $\hat{w}_1 \phi_1$ is the FLS to estimate nonlinearity. The Lyapunov function is selected and the derivation can be derived as follows:

$$V_e = \frac{1}{2} e_1^2 + \frac{1}{2} e_2^2 + \frac{1}{2} \tilde{w}_1^T \tilde{w}_1 \quad (40)$$

$$\begin{aligned} \dot{V}_e &= e_1 \dot{e}_1 + e_2 \dot{e}_2 + \tilde{w}_1^T \dot{w}_1 \\ &= e_1 (e_2 + \alpha_1) + e_2 (\theta \chi + \frac{1}{M} (f + g) \\ &\quad - \dot{\alpha}_1 + \theta u) + \tilde{w}_1^T \dot{w}_1 \\ &= -\lambda_1 e_1^2 - \lambda_2 e_2^2 \end{aligned} \quad (41)$$

where λ_1 , and λ_2 are positive constants. It is obvious that (41) is negative, which indicates that the system is asymptotic stable with fuzzy control law (38) and adaptive law (39). Next, considering the use of PPF in the adaptive fuzzy controller, we transform the coordinate of the system state $[x_{s1}, x_{s2}]$ as follow

$$\varepsilon_{s1} = \ln \left(\frac{a + \xi}{b - \xi} \right), \quad (\xi = \frac{x_{s1}}{\rho}) \quad (42)$$

$$\begin{aligned} \dot{\varepsilon}_{s1} &= \varepsilon_{s2} = \frac{a + b}{(a + \xi)(b - \xi)\rho} (\dot{x}_{s1} - x_{s1}\dot{\rho}/\rho) \\ &= r(x_{s2} - x_{s1}\dot{\rho}/\rho) \end{aligned} \quad (43)$$

$$\begin{aligned} \dot{\varepsilon}_{s2} &= \dot{r}(x_{s2} - x_{s1}\dot{\rho}/\rho) + r \left(\dot{x}_{s2} - \frac{x_{s2}\dot{\rho}}{\rho} - \frac{x_{s1}\ddot{\rho}}{\rho} + \frac{x_{s1}\dot{\rho}^2}{\rho^2} \right) \\ &= \dot{r}(x_{s2} - x_{s1}\dot{\rho}/\rho) - r \left(\frac{x_{s2}\dot{\rho}}{\rho} + \frac{x_{s1}\ddot{\rho}}{\rho} - \frac{x_{s1}\dot{\rho}^2}{\rho^2} \right) + r\dot{x}_{s2} \\ &= F + r\theta u \end{aligned} \quad (44)$$

where $a, b > 0$ are similarly defined as $\delta_{Li}, \delta_{Ui} (i = 1, 2, 3)$ in Section 3.1, $r = (a + b)/((a + \xi)(b - \xi)\rho)$ and $F = \dot{r}(x_{s2} - x_{s1}\dot{\rho}/\rho) - r(x_{s2}\dot{\rho}/\rho + x_{s1}\ddot{\rho}/\rho - x_{s1}\dot{\rho}^2/\rho^2) + r(\theta\chi + 1/M(f + g))$. ρ is exponentially decreasing function defined by PPF. Moreover, one can define the transformed system error as $s_1 = \varepsilon_{s1}$ and $s_2 = \varepsilon_{s2} - \alpha_2$, where α_2 is the intermediate virtual control and its expression is $\alpha_2 = -\gamma_1 s_1$. Then with the help of the FLS, the adaptive fuzzy controller with PPF can be designed as follows:

$$u = \frac{1}{r\theta} (-\gamma_2 s_2 - s_1 - \hat{w}_2 \phi_2 + \dot{\alpha}_2) \quad (45)$$

$$\dot{\hat{w}}_2 = -s_2 \phi_2 \quad (46)$$

where $\hat{w}_2 \phi_2$ is the FLS for estimating the nonlinearity F . The Lyapunov function is defined and its derivation is obtained as follows:

$$V_s = \frac{1}{2} s_1^2 + \frac{1}{2} s_2^2 + \frac{1}{2} \tilde{w}_2^T \tilde{w}_2 \quad (47)$$

$$\begin{aligned} \dot{V}_s &= s_1 \dot{s}_1 + s_2 \dot{s}_2 + \tilde{w}_2^T \dot{w}_2 \\ &= s_1 (s_2 + \alpha_2) + s_2 (F - \dot{\alpha}_2 + r\theta u) + \tilde{w}_2^T \dot{w}_2 \\ &= -\gamma_1 s_1^2 - \gamma_2 s_2^2 \end{aligned} \quad (48)$$

where γ_1, γ_2 are positive constant. Therefore \dot{V}_s is negative and the transformed system is asymptotic stable. Then under control (45), s_1 will converge to 0, thus $\xi \rightarrow (b - a)/2$ and $\dot{\xi} \rightarrow 0$. Besides, it should be noted that $\dot{\xi} = (x_{s2} - \xi\dot{\rho})/\rho$, ρ is the exponentially decreasing function and $\dot{\rho}$ is negative, thus the slope of ξ with respect to ξ is positive. Consequently, when $\xi > (b - a)/2$, then $\dot{\xi} > 0$ and when $\xi \leq (b - a)/2$, then $\dot{\xi} \leq 0$. Based on the inequality (37) and discussion above, we have

$$\begin{aligned} &\left| \ln \left(\frac{a + \xi}{b - \xi} \right) + \frac{a + b}{(a + \xi)(b - \xi)} \dot{\xi} \right| \\ &\geq \left| \frac{4}{a + b} \left(\xi - \frac{b - a}{2} \right) + \frac{4}{a + b} \dot{\xi} \right| \end{aligned} \quad (49)$$

Therefore, the salient convergence performance of adaptive fuzzy controller with PPF can be verified by comparing derivation (41) and (48), that is $\dot{V}_2 < \dot{V}_1 \Rightarrow \gamma_1 s_1^2 + \gamma_2 s_2^2 > k_1 e_1^2 + k_2 e_2^2$, which is represented by $F(\xi, \dot{\xi})$ subsequently. One can derive the following equation using inequality (37) and (49)

$$\begin{aligned} F(\xi, \dot{\xi}) &= \gamma_1 s_1^2 + \gamma_2 s_2^2 - \lambda_1 e_1^2 - \lambda_2 e_2^2 \\ &= \gamma_1 \left(\ln \left(\frac{a + \xi}{b - \xi} \right) \right)^2 + \gamma_2 \left(\frac{a + b}{(a + \xi)(b - \xi)} \dot{\xi} + \right. \\ &\quad \left. \gamma_1 \ln \left(\frac{a + \xi}{b - \xi} \right) \right)^2 - \lambda_1 (\rho \xi)^2 - \lambda_2 (\rho \dot{\xi} + (k_1 \rho + \dot{\rho}) \xi)^2 \\ &\geq \gamma_1 \left(\frac{4}{a + b} \left(\xi - \frac{b - a}{2} \right) \right)^2 + \gamma_2 \left(\gamma_1 \frac{4}{a + b} \left(\xi - \frac{b - a}{2} \right) \right. \\ &\quad \left. + \frac{4}{a + b} \dot{\xi} \right)^2 - \lambda_1 (\rho \xi)^2 - \lambda_2 ((\lambda_1 \rho + \dot{\rho}) \xi + \rho \dot{\xi})^2 \end{aligned} \quad (50)$$

Substituting $X = \xi$, $Y = \dot{\xi}$, $c = 4/(a + b)$, $d = (b - a)/2$, and $e = k_1 \rho + \dot{\rho}$, the above equation (50) can be further

deduced as:

$$\begin{aligned}
 & F(X, Y) \\
 & \geq \gamma_1 c^2 (X - d)^2 + \gamma_2 (\gamma_1 c (X - d) + cy)^2 \\
 & \quad - \lambda_1 \rho^2 x^2 - \lambda_2 (eX + \rho Y)^2 \\
 & = \gamma_1 c^2 (X - d)^2 + \gamma_2 [\gamma_1^2 c^2 (X - d)^2 + \\
 & \quad 2\gamma_1 c^2 (X - d)Y + c^2 Y^2] - \lambda_1 \rho^2 X^2 \\
 & \quad - \lambda_2 [e^2 X^2 + 2e\rho XY + \rho^2 Y^2] \\
 & = (\gamma_1 c^2 - \lambda_1 \rho^2) \left(X - \frac{\gamma_1 c^2 d}{2(\gamma_1 c^2 - \lambda_1 \rho^2)} \right)^2 \\
 & \quad + (\gamma_2 c^2 - \lambda_2 \rho^2) \left(Y + \frac{\gamma_1 \gamma_2 c^2 - \lambda_2 e\rho}{\gamma_2 c^2 - \lambda_2 \rho^2} X \right)^2 \\
 & \quad + \left(\gamma_2 \gamma_1^2 c^2 - \lambda_2 e^2 - \frac{(\gamma_1 \gamma_2 c^2 - \lambda_2 e\rho)^2}{(\gamma_2 c^2 - \lambda_2 \rho^2)} \right) X^2 \\
 & \quad - 2\lambda_2 dc^2 X - 2\lambda_2 cdeY + \lambda_2 c^2 d^2 \\
 & \quad - \frac{(\gamma_1 c^2)^2 d^2}{4(\gamma_1 c^2 - \lambda_1 \rho^2)} + \gamma_1 c^2 d^2
 \end{aligned} \tag{51}$$

The conditions to make (51) positive are that: 1) $(\gamma_1 c^2 - \lambda_1 \rho^2) = 16\gamma_1/(a+b)^2 - \lambda_1 \rho^2 \geq 0$; 2) $(\gamma_2 c^2 - \lambda_2 \rho^2) = 16\gamma_2/(a+b)^2 - \lambda_2 \rho^2 \geq 0$; 3) $(\gamma_2 \gamma_1^2 c^2 - \lambda_2 e^2 - (\gamma_1 \gamma_2 c^2 - \lambda_2 e\rho)^2 / (\gamma_2 c^2 - \lambda_2 \rho^2)) \geq 0$ and 4) $d = 0$ i.e., $a = b$. It is easy to meet the condition 4) because a, b are user-defined. Note that ρ is a function that decreases exponentially and eventually converges close to zero. Besides, $16\gamma_1/(a+b)^2$ and $16\gamma_2/(a+b)^2$ are positive constants. Consequently, conditions 1) and 2) always hold if $16\gamma_1/(a+b)^2 \geq \lambda_1 \rho_0^2$ and $16\gamma_2/(a+b)^2 \geq \lambda_2 \rho_0^2$, where ρ_0 is the initial value of ρ . As for condition 3), one can obtain that

$$\begin{aligned}
 & \left(\gamma_2 \gamma_1^2 c^2 - \lambda_2 e^2 - \frac{(\gamma_1 \gamma_2 c^2 - \lambda_2 e\rho)^2}{(\gamma_2 c^2 - \lambda_2 \rho^2)} \right) \\
 & = \frac{16(\rho_1(\gamma_1 - \lambda_1) + \rho_1)^2 \gamma_2 \lambda_2}{(a+b)^2 \lambda_2 \rho^2 - 16\gamma_2},
 \end{aligned}$$

and owing to the property of ρ , the condition 3) converges to zero. Also, one can set the parameter γ_1 close to λ_1 .

In conclusion, the equation (51) is positive when the four above-mentioned conditions are satisfied; then the derivation (48) is smaller than (41), which indicates that the convergence rate of the system under adaptive fuzzy control with PPF is greater than the one without.

Remark 5 For the first time, this paper theoretically proves the superior convergence performance of PPF. The result can guide the design of the controller with PPF. It should be noted that the four conditions mentioned above are based on the internal properties of PPF parameters, such as ρ . Its exponential decrease characteristic determines the salient convergence performance.

Though the convergence performance of the controller involved PPF is proved better, it still involves the FLS during the design. Thus, there is a need to discuss further the convergence property of the approximation-free controller involving PPF. Next, the convergence performance of the approximation-free controller proposed in this paper in comparison to the adaptive fuzzy controller (38) will be analyzed theoretically. According to the above analysis, it is ideal to set $a = b$,

i.e., $\delta_{Li} = \delta_{Ui}, i = 1, 2, 3$. From Section 3.2, one can obtain the derivation of Lyapunov function about relative suspension system under proposed control method as follows:

$$\begin{aligned}
 \dot{V}_\varepsilon & = \dot{V}_1 + \dot{V}_2 + \dot{V}_3 \\
 & \leq -r_1(k_1 \varepsilon_1^2 - Q_1 |\varepsilon_1|) - r_2(k_2 \varepsilon_2^2 - Q_2 |\varepsilon_2|) \\
 & \quad - r_3(k_3 \varepsilon_3^2 - Q_3 |\varepsilon_3|)
 \end{aligned} \tag{52}$$

Based on the knowledge in Section 3.2, one can get that $\xi_3 = (x_2 - u_2)/\rho_3$, ($u_2 = -(k_2/\theta) \varepsilon_2$) and $x_2 = \xi_2 \rho_2 + u_1 + y_2 + x_4$, ($u_1 = -k_1 \varepsilon_1$). By virtue of inequality (37) and $AB \leq (A^2 + B^2)/2$, the third term on the right side of (52) is further expressed as:

$$\begin{aligned}
 & r_3(k_3 \varepsilon_3^2 - Q_3 |\varepsilon_3|) \\
 & \geq 2r_3 \left(\frac{2k_3 - 1}{a^2} \right) \xi_3^2 - \frac{1}{2} r_3 Q_3^2 \\
 & = \beta (x_2^2 - 2x_2 u_2 + u_2^2) - \frac{1}{2} r_3 Q_3^2 \\
 & = \beta u_2^2 + \beta u_1^2 + 2\beta (\xi_2 \rho_2 + y_2 + x_4) \\
 & \quad + \beta (\xi_2 \rho_2 + y_2 + x_4)^2 - 2\beta x_2 u_2 - \frac{1}{2} r_3 Q_3^2 \\
 & = \beta (k_2/\theta)^2 \varepsilon_2^2 + \beta k_1^2 \varepsilon_1^2 + 2\beta \Delta u_1 \\
 & \quad + \beta \Delta^2 - 2\beta x_2 u_2 - \frac{1}{2} r_3 Q_3^2
 \end{aligned} \tag{53}$$

wherein, $\beta = 2r_3(2k_3 - 1)/(a^2 \rho_3^2)$ and $\Delta = \xi_2 \rho_2 + y_2 + x_4$. Then subtracting (41) from (52), substituting (53), and utilizing inequality (37), the following equation is derived

$$\begin{aligned}
 & \left| \dot{V}_\varepsilon \right| - \left| \dot{V}_z \right| \\
 & = r_1(k_1 \varepsilon_1^2 - \bar{Q}_1 |\varepsilon_1|) + r_2(k_2 \varepsilon_2^2 - \bar{Q}_2 |\varepsilon_2|) \\
 & \quad + r_3(k_3 \varepsilon_3^2 - \bar{Q}_3 |\varepsilon_3|) - \lambda_1 e_1^2 - \lambda_2 e_2^2 \\
 & \geq r_1 \left(\frac{4k_1}{a^2} \xi_1^2 - \bar{Q}_1 |\varepsilon_1| \right) + r_2 \left(\frac{4k_2}{a^2} \xi_2^2 - \bar{Q}_2 |\varepsilon_2| \right) \\
 & \quad - \lambda_1 \rho_1^2 \xi_1^2 - \lambda_2 (\lambda_1 \rho_1 \xi_1 - k_1 \varepsilon_1 + \rho_2 \xi_2)^2 \\
 & \quad + r_3(k_3 \varepsilon_3^2 - \bar{Q}_3 |\varepsilon_3|) \\
 & = \left(\frac{4k_1 r_1}{a^2} - \lambda_1^2 \lambda_2 \rho_1^2 - \lambda_1 \rho_1^2 \right) \xi_1^2 - 2\lambda_1 \lambda_2 \rho_1 \rho_2 \xi_1 \xi_2 \\
 & \quad + \left(\frac{4k_2 r_2}{a^2} - \lambda_2 \rho_2^2 \right) \xi_2^2 - \lambda_2 k_1^2 \varepsilon_1^2 \\
 & \quad + (2k_1 \lambda_1 \lambda_2 \rho_1 \xi_1 + 2k_1 \lambda_2 \rho_2 \xi_2) \varepsilon_1 - r_1 \bar{Q}_1 |\varepsilon_1| \\
 & \quad - r_2 \bar{Q}_2 |\varepsilon_2| + r_3(k_3 \varepsilon_3^2 - \bar{Q}_3 |\varepsilon_3|) \\
 & = \left(\frac{4k_1 r_1}{a^2} - \lambda_1^2 \lambda_2 \rho_1^2 - \lambda_1 \rho_1^2 \right) (\xi_1 - \eta \xi_2)^2 \\
 & \quad + \left(\frac{4k_2 r_2}{a^2} - \lambda_2 \rho_2^2 - \mu \right) \xi_2^2 + (\lambda_2 k_1^2 + \beta k_1^2) \varepsilon_1^2 \\
 & \quad - (2\beta k_1 \bar{\Delta} + r_1 \bar{Q}_1) |\varepsilon_1| + \beta (k_2/\theta)^2 \varepsilon_2^2 \\
 & \quad - (2\beta (k_2/\theta) \bar{x}_2 + r_2 \bar{Q}_2) |\varepsilon_2| + \beta \Delta^2 - \frac{1}{2} r_3 \bar{Q}_3^2
 \end{aligned} \tag{54}$$

wherein, $\bar{\Delta} = \sup \{|\Delta|\}$, $\bar{x}_2 = \sup \{|x_2|\}$, $\eta = \lambda_1 \lambda_2 \rho_1 \rho_2 a^2 / (4r_1 k_1 - a^2 \lambda_1^2 \lambda_2 \rho_1^2 - a^2 \lambda_1 \rho_1^2)$ and $\mu = \lambda_1^2 \lambda_2^2 \rho_1^2 \rho_2^2 a^2 / (4r_1 k_1 - a^2 \lambda_1^2 \lambda_2 \rho_1^2 - a^2 \lambda_1 \rho_1^2)$. Thus, from the equation (54), it can be inferred that the conditions $4r_1 k_1/a^2 - \lambda_1^2 \lambda_2 \rho_1^2 - \lambda_1 \rho_1^2 \geq 0$

TABLE I
PARAMETERS OF SUSPENSION SYSTEM [32]

Parameter	Value	Parameter	Value
m_s	240kg	k_t	23.61kg
m_u	15394N/m	c_t	1385.4Ns/m
k_{s1}	-73696N/m	c_{s1}	524.28Ns/m
k_{s2}	3170400N/m	c_{s2}	13.8Ns/m
k_{s3}	181818.88N/m		

TABLE II
PARAMETERS OF BIOINSPIRED MODEL [32]

Parameter	Value	Parameter	Value
M	240kg	k_v	250N/m
L_1	0.1m	k_h	500N/m
L_2	0.2m	μ_1	1Ns/m
θ_1	$\pi/6$ rad	μ_2	0.155Ns/m

and $4r_2k_2/a^2 - \lambda_2\rho_2^2 - \mu \geq 0$ are always satisfied if they are satisfied at initial position, i.e., at $r_1 = r_{10}, r_2 = r_{20}, \rho_1 = \rho_{10}, \rho_2 = \rho_{20}$, owing to the exponentially decrease property of ρ_1 and ρ_2 . In addition, it is obvious that $\lambda_2k_1^2 + \beta k_1^2$ and $\beta(k_2/\theta)^2$ in (54) are positive. Then, with the knowledge that $\varepsilon_1 > \bar{Q}_1/k_1$, $\varepsilon_2 > \bar{Q}_2/k_2$ and $\varepsilon_3 > \bar{Q}_3/k_3$ provided in Section 3.2, one can deduce the following conditions

$$\frac{(2\beta\bar{\Delta}k_1 + r_1\bar{Q}_1)}{(\lambda_2 + \beta)k_1^2} \leq \frac{\bar{Q}_1}{k_1} \Rightarrow \frac{2\beta k_1\bar{\Delta}}{(\lambda_2 + \beta)k_1 - r_1} \leq \bar{Q}_1$$

$$\frac{(2\beta(k_2/\theta)\bar{x}_2 + r_2\bar{Q}_2)}{\beta(k_2/\theta)^2} \leq \frac{\bar{Q}_2}{k_2} \Rightarrow \frac{2\beta(k_2/\theta)\bar{x}_2}{\beta(k_2/\theta^2) - r_2} \leq \bar{Q}_2.$$

Furthermore, the last term of (54) indicates that if $\beta\Delta^2 - r_3\bar{Q}_3^2/2 \geq 0$ is satisfied, β needs to be appropriately chosen a large value. The convergence performance analysis above helps to choose proper parameters in subsequent simulation.

IV. SIMULATION AND DISCUSSION

Specific examples are presented to verify the feasibility and superiority of the proposed controller and the comparison between the proposed controller and another controller is executed here. In order to facilitate subsequent simulation and comparison, the unknown nonlinear terms in the suspension system (1) are given as follow

$$F_s = k_{s1}(z_s - z_u) + k_{s2}(z_s - z_u)^2 + k_{s3}(z_s - z_u)^3$$

$$F_d = c_{s1}(\dot{z}_s - \dot{z}_u) + c_{s2}(\dot{z}_s - \dot{z}_u)^2 \quad (55)$$

wherein k_{s1} is linear stiffness coefficient; k_{s2} and k_{s3} are nonlinear stiffness coefficients; c_{s1} and c_{s2} are damping coefficients of nonlinear dampers; k_t and c_t denote stiffness coefficient and damping coefficient of the tire, respectively.

Moreover, to verify the superiority, the fuzzy adaptive control (FAC) based on the bioinspired model for a suspension system in [31] is compared to the controller proposed in this paper. The parameters of the suspension system and bioinspired reference model are given in Table I and Table II.

Three types of road excitation were used here: random road, bump road, and sinusoidal road. The random road was

TABLE III
ACCELERATION RMS OF SUSPENSION SYSTEMS WITH DIFFERENT CONTROLLERS (M/S²)

V	Passive	FAC[31]	Proposed
$V_1 = 20km/h$	0.116	0.0292(↓74.82%)	0.0240(↓79.31%)
$V_2 = 40km/h$	0.164	0.0413(↓74.82%)	0.0342(↓79.15%)
$V_3 = 60km/h$	0.2009	0.0506(↓74.81%)	0.0419(↓79.14%)
$V_4 = 100km/h$	0.2593	0.0655(↓74.74%)	0.0542(↓79.10%)

TABLE IV
COMPUTATIONAL TIME (S)

V	FAC[31]	Proposed
$V_1 = 20km/h$	204.5893	44.5253(↓78.24%)
$V_2 = 40km/h$	204.4992	45.7517(↓77.63%)
$V_3 = 60km/h$	205.3395	44.8423(↓78.16%)
$V_4 = 100km/h$	204.3396	45.9872(↓77.49%)

used to verify the vibration suppression performance of the proposed control method, and bump road and sinusoidal road were utilized to show the transient performance.

A. Random Road

The random excitation is present as follow

$$\dot{z}_r(t) = -2\pi n_z V z_r(t) + 2\pi n_0 \sqrt{G_z(n_0)} V \omega(t) \quad (56)$$

where $n_z = 0.0001$, $n_0 = 0.1$ and $G_z(n_0) = 256 \times 10^{-6}$; $\omega(t)$ is the standard Gaussian white noise with 0 mean and unit variance and V is the longitudinal velocity of the vehicle. Four different velocities were set, i.e., $V = 20km/h$, $V = 40km/h$, $V = 60km/h$, and $V = 100km/h$ for subsequent simulation. The whole simulation time was taken as 50s.

The initial states of the system were all set as zero. Parameters of the proposed controller were chosen through the trial-and-error method. Hence, control gains were set as $k_1 = 0.01$, $k_2 = 0.083$ and $k_3 = 0.834$. Parameters of tanh function were defined as $\delta_{L1} = \delta_{U1} = \delta_{L2} = \delta_{U2} = \delta_{L3} = \delta_{U3} = 1$ and prescribed performance functions were given as follows:

$$\rho_1 = (0.001 - 0.0001)e^{-17t} + 0.0001$$

$$\rho_2 = (0.55 - 0.1)e^{-15t} + 0.1$$

$$\rho_3 = (1.1 - 0.95)e^{-12t} + 0.95$$

TABLE V
ACCELERATION RMS UNDER DIFFERENT CONTROLLERS WITH DISTURBANCE (M/S²)

V	Passive	FAC[31]	Proposed
$V_1 = 20km/h$	1.225	0.0662(↓94.60%)	0.0454(↓96.29%)
$V_2 = 40km/h$	1.2306	0.0745(↓93.95%)	0.0522(↓95.76%)
$V_3 = 60km/h$	1.2363	0.0819(↓93.38%)	0.0582(↓95.29%)
$V_4 = 100km/h$	1.2478	0.0952(↓92.37%)	0.0692(↓94.45%)

TABLE VI
COMPUTATIONAL TIME WITH DISTURBANCE (S)

V	FAC[31]	Proposed
$V_1 = 20km/h$	337.7891	53.6581(↓84.11%)
$V_2 = 40km/h$	340.0640	51.5062(↓84.85%)
$V_3 = 60km/h$	338.2901	50.8201(↓84.98%)
$V_4 = 100km/h$	341.2300	52.7526(↓84.54%)

To evaluate the vibration isolation performance of different controllers, the root-mean-square (RMS) was used as the evaluation criteria. The general form can be described as follows:

$$RMS(\chi) = \sqrt{\frac{1}{T} \int_0^T \chi^2 dt} \quad (57)$$

Only the time history diagram of sprung mass acceleration with different controllers when $V = 100km/h$ is shown in Fig 4 as the representative (similar trends were observed for the other three groups of velocities) and corresponding acceleration RMSs of suspension system controlled by different controllers in different velocities are listed in Table III, where the passive suspension system is the reference. In Fig 4, the blue, red and yellow lines represent the acceleration produced by the passive suspension system, suspension with FAC, and suspension with the proposed controller, respectively. From Fig 4, it can be concluded that both two controllers effectively suppressed the vibration compared to the passive suspension system and the acceleration of the suspension system with the proposed control method decreased more than that could be achieved with the FAC, which can be further verified in Table III. The proposed controller reduces the RMS of acceleration more than FAC even when velocity varies, which indicates better vibration suppression. Besides, the actual time taken by the suspension systems with different controllers is given in Table IV. Compared to the suspension system with FAC, the one with the proposed control method significantly reduces the computational time, which illustrates the simplicity of the proposed controller.

As safety and comfort improvement must be guaranteed, the suspension system should satisfy the constraints (4) and (5) mentioned above in Section 2. The situation during the maximum velocity $V = 100km/h$ is analyzed representatively here. The maximum suspension deflection is $z_{max} = 0.1m$. The dynamic tyre load and suspension deflection are shown in Fig 5 (a, b), wherein the rate represents the dynamic tyre load $(F_t + F_b)/(m_s + m_u)g$. From Fig 5, it is clear that both indexes are in the acceptable range, proving that the proposed controller improve the suspension system's comfort and ensures safety simultaneously.

In order to demonstrate the robustness of the proposed controller, the disturbance $w = \sin(3\pi t) + 0.2\sin(30\pi t)$ is introduced into sprung mass in (1). The same random road excitation is used, and the same four forward velocities are chosen, then the comparison of acceleration RMS and computational time under different controllers are presented in Table V and Table VI, respectively, when disturbance exists. FAC and the proposed controller can resist disturbance, as shown in Table 5. Furthermore, the proposed control method performs better than FAC in suppressing the vibration during various velocities when disturbance exists, which illustrates the better robustness of proposed controller. From Table VI, the conclusion can be made that the proposed controller's computational time is still less than FAC's. Besides, the reduction in computational time with disturbance situation is more than the reduction in computational time without disturbance, which further indicates the superior robustness

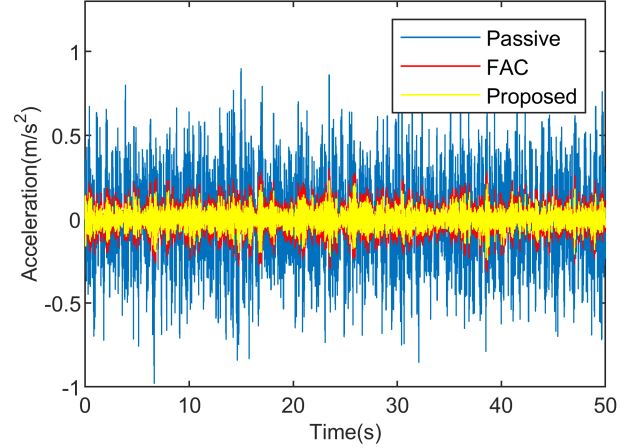


Fig. 4. Acceleration of suspension systems with different controllers for $V = 100km/h$

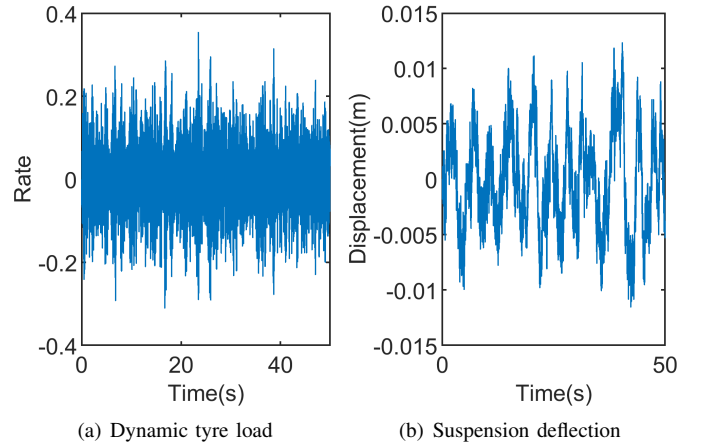


Fig. 5. Acceleration of suspension systems under different controllers when $V = 100km/h$

of the proposed controller.

In addition, to testify the adaptation of the proposed control method to uncertainty, the simulation is executed when the sprung mass varies from 210kg to 270kg in the interval of 10 kg. Using the same random road with the forward velocity $V = 100km/h$, the result is shown in Fig 6, wherein the Proposed-rate and FAC-rate express the ratio of the acceleration RMS under the proposed scheme and FAC respected to the one of passive suspension, respectively. It is evident that all acceleration RMSs with different suspension system settings (Proposed, FAC, Passive) decrease with the increase of sprung mass, but the proposed controller still performs better in suppressing vibration compared to FAC, implying that the proposed controller is more adaptive to uncertainty.

B. Bump Road

The simulation is implemented under bump road excitation to verify the convergence performance of the proposed con-

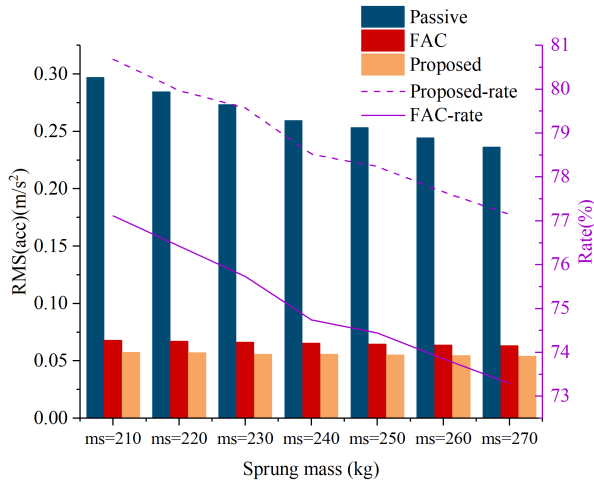


Fig. 6. RMS of acceleration with sprung mass changing

troller. The following equation expresses the bump road.

$$z_r(t) = \begin{cases} l \frac{\alpha}{4} (1 - \cos(\frac{2\pi V}{l} t)), & 0 \leq t \leq \frac{l}{V} \\ 0, & t > \frac{l}{V} \end{cases} \quad (58)$$

where a , l are the height and length of the bump, which is set as $\alpha = 0.1m$, $l = 5m$, and V is the forward velocity, which is chosen as $V = 40km/h$. The initial states of the system are set as $[x_1, x_2, x_3, x_4] = [0.06, 0, 0, 0]$, and $[y_1, y_2] = [0, 0]$. The control parameters are given as follows: $k_1 = 3$, $k_2 = 0.033$, $k_3 = 4.167$ and tanh function parameters are selected as $\delta_{L1} = \delta_{U1} = \delta_{L2} = \delta_{U2} = \delta_{L3} = \delta_{U3} = 1$. Prescribed performance functions are determined as

$$\begin{aligned} \rho_{U1} &= (0.1 - 0.0001)e^{-8t} + 0.0001, \rho_{L1} = 0.0001 \\ \rho_2 &= (1 - 0.01)e^{-5t} + 0.01 \\ \rho_3 &= (12.5 - 0.5)e^{-1t} + 0.5. \end{aligned}$$

The responses of the suspension system to bump excitation under the control of the FAC and the proposed method are depicted in Fig 7 and Fig 8, where the response of the passive suspension system is to demonstrate the control's effect more clearly. The absolute displacement x_1 is shown in Fig 7 and the corresponding velocity x_2 in Fig 8. It can be concluded from Fig 7 that both control methods are effective to stabilize the suspension system to a small residual set as soon as possible and eliminate the fluctuation when bump excitation occurs. Moreover, the proposed method has a faster response than FAC, as shown in Fig 7, and the velocity x_2 in Fig 8 also proves the conclusion in another way. The tracking error displayed in Fig 9 further indicates the faster convergence of the proposed method. In Fig 9, the green dotted line is the tracking error convergence boundary preset by the prescribed performance function. The tracking error under the proposed controller is within the convergence boundary for the entire time, while a part of the tracking error under the FAC does not, which indicates that the proposed controller can confine

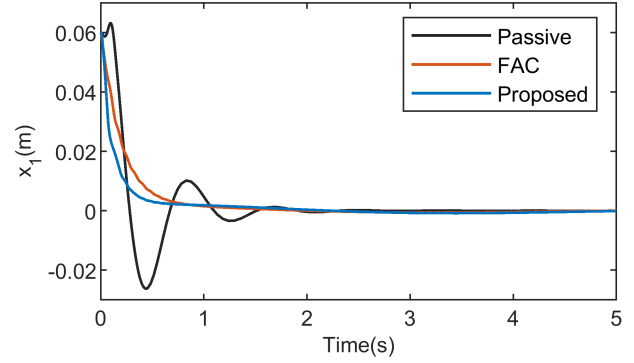


Fig. 7. Suspension system's response x_1 in bump road

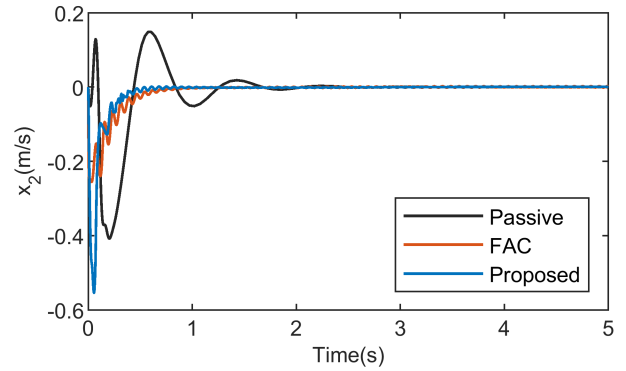


Fig. 8. Suspension system's response x_2 in bump road

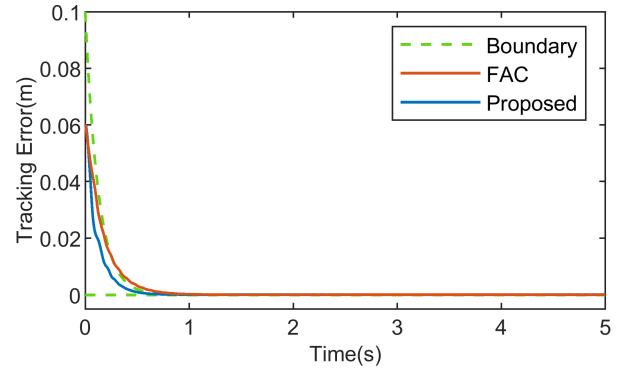


Fig. 9. Comparison of convergence performance between FAC and proposed controller in bump road

the tracking error in the prescribed range. Moreover, it can be seen from Fig 9 that the convergence rate of the system signal controlled by the proposed method is greater than that of FAC. This merit can be further demonstrated in sinusoidal road subsequently.

C. Sinusoidal Road

The sinusoidal excitation is expressed as $z_r = 0.025 \sin(2\pi t)$. The initial states of the system are the same as that in the bump road. The control parameters are set as: $k_1 = 3$, $k_2 = 0.033$, $k_3 = 4.167$ and tanh function parameters are $\delta_{L1} = \delta_{U1} = \delta_{L2} = \delta_{U2} = \delta_{L3} = \delta_{U3} = 1$.

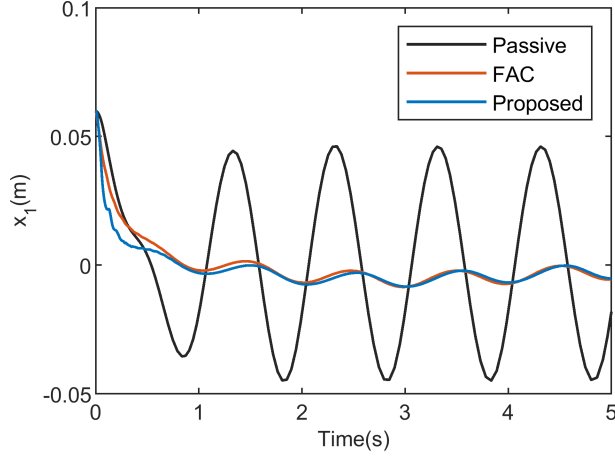


Fig. 10. Suspension system's response x_1 in sinusoidal road

Prescribed performance functions are chosen as

$$\begin{aligned}\rho_{U1} &= (0.1 - 0.0001)e^{-7t} + 0.0001, \rho_{L1} = 0.0001 \\ \rho_2 &= (1 - 0.01)e^{-5t} + 0.01 \\ \rho_3 &= (12.5 - 0.5)e^{-1t} + 0.5\end{aligned}$$

The responses of the passive suspension and the suspension under the control of FAC and the proposed controller to sinusoidal excitation are described, and the absolute displacement x_1 is displayed in Fig 10 and the corresponding velocity x_2 in Fig 11. The results show the effectiveness of both two controllers in stabilizing the system and reducing fluctuation caused by sinusoidal excitation and the faster response of the proposed method can be seen when comparing the results in Fig 10 and Fig 11. The further validation is in Fig 12, which shows the tracking error of different controllers. The green dotted line has the same definition as mentioned in the bump road case. From Fig 12, it can also be deduced that the proposed controller has a greater convergence rate than FAC. Moreover, it should be noted that the proposed method has a more precise tracking error than FAC, since the tracking error controlled by FAC violates the prescribed bound during the stable region while controlled by the proposed controller does not. It further indicates that the proposed controller possesses better convergence performance than FAC.

V. CONCLUSION

In this paper, a novel control scheme was proposed for a suspension system with uncertainty and unknown nonlinearity. The control scheme consisted two parts: one was the bio-inspired model, and another one was the approximation-free control scheme. It has been proved by Lyapunov Theorem that the suspension system could be stabilized by the proposed control scheme. Main conclusions can be drawn from this work, as follows: Firstly, the significant computational time was reduced and the better vibration suppression performance was obtained without compromising ride safety, simultaneously. The proposed controller had a similar recursion scheme as backstepping control, but without adaptive law. Furthermore,

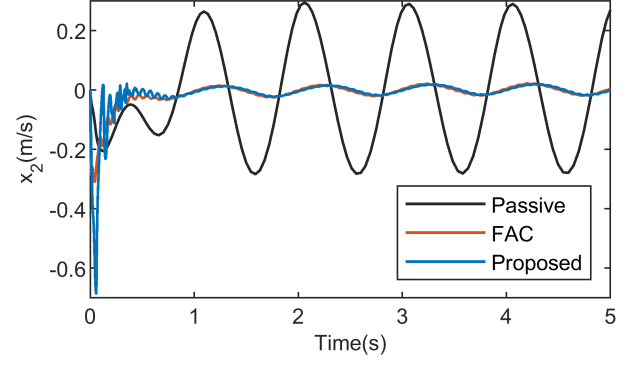


Fig. 11. Suspension system's response x_2 in sinusoidal road

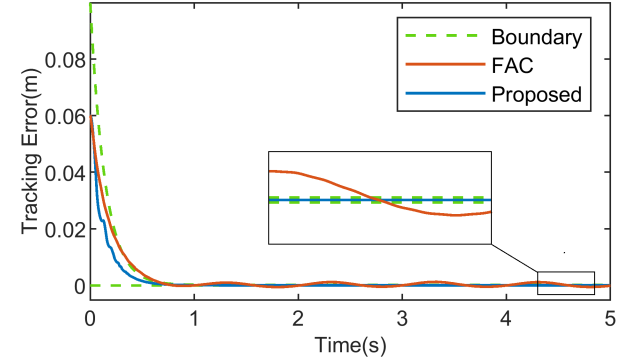


Fig. 12. Comparison of convergence performance between FAC and proposed controller in sinusoidal road

the approximation functions (FLS or NNs) were avoided. Then it resulted in a simpler structure and less computational time. The nonlinearity inside the bio-inspired model benefited in vibration suppression, then the ideal trajectory was produced and assisted the controller to suppress excess vibration. Moreover, a comparison simulation of time consumption and acceleration with or without disturbance and changeable passengers was conducted to justify the conclusion above. The results indicated the better vibration suppression performance, robustness, and simple structure of the proposed controller. Secondly, the assistance of the PPF involved in the proposed controller achieved better transient performance. The exponentially decreased characteristic of PPF promoted the convergence rate and arrived at a more precise tracking error. The theoretical comparison and analysis among these controllers with and without PPF have been investigated, which confirmed the second conclusion. Moreover, comparison simulation carried in bump and sinusoidal road further verified the conclusion. The results illustrated the faster convergence and more precise response of proposed control scheme. In addition, this study process considered the safety and comfort requirements for the suspension system. It should be noted that the singularity of the approximation-free control remains still and many control parameters need to be determined synthetically by trial and error. Future work will integrate other control methods to solve the singularity problem and utilize optimization methods to design control parameters.

ACKNOWLEDGMENT

This work was supported by the National Natural Science Foundation of China (No. 11832009). The authors would like to express their gratitude to EditSprings (<https://www.editsprings.com/>) for the expert linguistic services provided.

APPENDIX I

BIOINSPIRED MODEL'S FORCE ANALYSIS

The dynamic analysis and the proof of Lemma 1 are given here. As Fig 3 shown, the main force loads in joint 2. The force condition is analyzed in joint 1, joint 2 and joint 3, respectively. Then, we have the following equations satisfied.

$$f = k_v y_r + \frac{k_h}{2} (L_1 \cos \theta_1 + L_2 \cos \theta_2 - \sqrt{L_1^2 - v^2(y_r)} - \sqrt{L_2^2 - v^2(y_r)}) \cdot \left(\frac{v^2(y_r)}{\sqrt{L_1^2 - v^2(y_r)}} + \frac{v^2(y_r)}{\sqrt{L_2^2 - v^2(y_r)}} \right) \quad (A1)$$

where $v(y_r) = L_1 \sin \theta_1 + y_r/2$. Then, according to the Lagrange principle, one can deduce the state-space equation (8) for the bioinspired model by following kinetic energy (A2) and potential energy (A3) and Hamilton function (A4)

$$T = \frac{1}{2} M \dot{y}^2 \quad (A2)$$

$$V = \frac{1}{2} k_h x^2 + \frac{1}{2} k_v (y_r - \Delta y)^2 + M g y \quad (A3)$$

$$\frac{d}{dt} \left(\frac{\partial L}{\partial \dot{y}} \right) - \frac{\partial L}{\partial y} = -\mu_1 \dot{y}_r - \mu_2 n_x \dot{\varphi} \frac{\partial \varphi}{\partial y} \quad (A4)$$

where Δy is the vertical spring compressive deflection and x satisfies that $x = x_1 + x_2$. In Hamilton function, L and φ satisfy $L = T - V$ and $\varphi = \varphi_1 + \varphi_2$, respectively. n_x is the number of joints. μ_1 and μ_2 are the air damping coefficient and rotational friction coefficient, respectively.

REFERENCES

- [1] G. Yan, M. Fang, and J. Xu, "Analysis and experiment of time-delayed optimal control for vehicle suspension system," *Journal of Sound and Vibration*, vol. 446, pp. 144–158, 2019.
- [2] D. Jing, J.-Q. Sun, C.-B. Ren, and X.-h. Zhang, "Multi-objective optimization of active vehicle suspension system control," pp. 137–145, Cham: Springer International Publishing, 2020.
- [3] H. Li, X. Jing, and H. R. Karimi, "Output-feedback-based h_∞ control for vehicle suspension systems with control delay," *IEEE Transactions on Industrial Electronics*, vol. 61, no. 1, pp. 436–446, 2014.
- [4] H. Du and N. Zhang, "control of active vehicle suspensions with actuator time delay," *Journal of Sound and Vibration*, vol. 301, no. 1-2, pp. 236–252, 2007.
- [5] J. Wu, Z. Liu, and W. Chen, "Design of a piecewise affine h_∞ controller for mr semiactive suspensions with nonlinear constraints," *IEEE Transactions on Control Systems Technology*, vol. 27, no. 4, pp. 1762–1771, 2019.
- [6] L.-X. Guo and L.-P. Zhang, "Robust h_∞ control of active vehicle suspension under non-stationary running," *Journal of Sound and Vibration*, vol. 331, no. 26, pp. 5824–5837, 2012.
- [7] J. J. Rath, M. Defoort, H. R. Karimi, and K. C. Veluvolu, "Output feedback active suspension control with higher order terminal sliding mode," *IEEE Transactions on Industrial Electronics*, vol. 64, no. 2, pp. 1392–1403, 2017.
- [8] H. Pang, X. Zhang, J. Yang, and Y. Shang, "Adaptive backstepping-based control design for uncertain nonlinear active suspension system with input delay," *International Journal of Robust and Nonlinear Control*, vol. 29, no. 16, pp. 5781–5800, 2019.
- [9] W. Sun, H. Gao, and O. Kaynak, "Adaptive backstepping control for active suspension systems with hard constraints," *IEEE/ASME Transactions on Mechatronics*, vol. 18, no. 3, pp. 1072–1079, 2013.
- [10] R. Zhao, W. Xie, P. K. Wong, D. Cabecinhas, and C. Silvestre, "Adaptive vehicle posture and height synchronization control of active air suspension systems with multiple uncertainties," *Nonlinear Dynamics*, vol. 99, no. 3, pp. 2109–2127, 2020.
- [11] Y.-J. Liu, Y. Zhang, L. Liu, S. Tong, and C. L. P. Chen, "Adaptive finite-time control for half-vehicle active suspension systems with uncertain dynamics," *IEEE/ASME Transactions on Mechatronics*, vol. 26, pp. 168–178, 2021.
- [12] Y.-J. Liu, Q. Zeng, S. Tong, C. L. P. Chen, and L. Liu, "Adaptive neural network control for active suspension systems with time-varying vertical displacement and speed constraints," *IEEE Transactions on Industrial Electronics*, vol. 66, no. 12, pp. 9458–9466, 2019.
- [13] L. Liu, X. Li, Y.-J. Liu, and S. Tong, "Neural network based adaptive event trigger control for a class of electromagnetic suspension systems," *Control Engineering Practice*, vol. 106, 2021.
- [14] J. Na, Y. Huang, X. Wu, S.-F. Su, and G. Li, "Adaptive finite-time fuzzy control of nonlinear active suspension systems with input delay," *IEEE Transactions on Cybernetics*, vol. 50, no. 6, pp. 2639–2650, 2020.
- [15] O. Demir, I. Keskin, and S. Cetin, "Modeling and control of a nonlinear half-vehicle suspension system: a hybrid fuzzy logic approach," *Nonlinear Dynamics*, vol. 67, no. 3, pp. 2139–2151, 2012.
- [16] M. E. Shalabi, A. M. R. Fath Elbab, H. El-Hussieny, and A. A. Abouelsoud, "Neuro-fuzzy volume control for quarter car air-spring suspension system," *IEEE access*, vol. 9, pp. 77611–77623, 2021.
- [17] N. Al-Holou, T. Lahdhiri, D. S. Joo, J. Weaver, and F. Al-Abbas, "Sliding mode neural network inference fuzzy logic control for active suspension systems," *IEEE transactions on fuzzy systems*, vol. 10, no. 2, pp. 234–246, 2002.
- [18] S.-J. Huang and W.-C. Lin, "Adaptive fuzzy controller with sliding surface for vehicle suspension control," *IEEE transactions on fuzzy systems*, vol. 11, no. 4, pp. 550–559, 2003.
- [19] C. P. Bechlioulis and G. A. Rovithakis, "Adaptive control with guaranteed transient and steady state tracking error bounds for strict feedback systems," *Automatica*, vol. 45, no. 2, pp. 532–538, 2009.
- [20] C. P. Bechlioulis and G. A. Rovithakis, "Robust adaptive control of feedback linearizable mimo nonlinear systems with prescribed performance," *IEEE Transactions on Automatic Control*, vol. 53, no. 9, pp. 2090–2099, 2008.
- [21] C. P. Bechlioulis and G. A. Rovithakis, "Robust partial-state feedback prescribed performance control of cascade systems with unknown nonlinearities," *IEEE Transactions on Automatic Control*, vol. 56, no. 9, pp. 2224–2230, 2011.
- [22] G. A. R. Charalampos P. Bechlioulis, "A low-complexity global approximation-free control scheme with prescribed performance for unknown pure feedback systems," *Automatica*, 2014.
- [23] Y. Huang, J. Na, X. Wu, and G. Gao, "Approximation-free control for vehicle active suspensions with hydraulic actuator," *IEEE Transactions on Industrial Electronics*, vol. 65, no. 9, pp. 7258–7267, 2018.
- [24] Y. Huang, J. Na, X. Wu, X. Liu, and Y. Guo, "Adaptive control of nonlinear uncertain active suspension systems with prescribed performance," *ISA Transactions*, vol. 54, pp. 145–155, 2015.
- [25] J. Na, Y. Huang, X. Wu, G. Gao, G. Herrmann, and J. Z. Jiang, "Active adaptive estimation and control for vehicle suspensions with prescribed performance," *IEEE Transactions on Control Systems Technology*, vol. 26, no. 6, pp. 2063–2077, 2018.
- [26] J. Na, "Adaptive prescribed performance control of nonlinear systems with unknown dead zone," *International Journal of Adaptive Control and Signal Processing*, vol. 27, no. 5, pp. 426–446, 2013.
- [27] J. Na, Q. Chen, X. Ren, and Y. Guo, "Adaptive prescribed performance motion control of servo mechanisms with friction compensation," *IEEE Transactions on Industrial Electronics*, vol. 61, no. 1, pp. 486–494, 2014.
- [28] F. Jia, C. Lei, J. Lu, and Y. Chu, "Adaptive prescribed performance output regulation of nonlinear systems with nonlinear exosystems," *International Journal of Control, Automation and Systems*, vol. 18, no. 8, pp. 1946–1955, 2020.
- [29] R. Zhang, B. Xu, and W. Zhao, "Finite-time prescribed performance control of mems gyroscopes," *Nonlinear Dynamics*, vol. 101, no. 4, pp. 2223–2234, 2020.
- [30] H. Pan, X. Jing, W. Sun, and H. Gao, "A bioinspired dynamics-based adaptive tracking control for nonlinear suspension systems," *IEEE*

- Transactions on Control Systems Technology*, vol. 26, no. 3, pp. 903–914, 2018.
- [31] Z. Wu, X. Jing, J. Bian, F. Li, and R. Allen, “Vibration isolation by exploring bio-inspired structural nonlinearity,” *Bioinspiration & biomimetics*, vol. 10, no. 5, pp. 056015–056015, 2015.
- [32] J. Li, X. Jing, Z. Li, and X. Huang, “Fuzzy adaptive control for nonlinear suspension systems based on a bioinspired reference model with deliberately designed nonlinear damping,” *IEEE Transactions on Industrial Electronics*, vol. 66, no. 11, pp. 8713–8723, 2019.
- [33] M. Zhang and X. Jing, “A bioinspired dynamics-based adaptive fuzzy smc method for half-car active suspension systems with input dead zones and saturations,” *IEEE Transactions on Cybernetics*, vol. 51, no. 4, pp. 1743–1755, 2021.
- [34] M. Zhang, X. Jing, and G. Wang, “Bioinspired nonlinear dynamics-based adaptive neural network control for vehicle suspension systems with uncertain/ unknown dynamics and input delay,” *IEEE Transactions on Industrial Electronics*, pp. 1–10, 2020.
- [35] E. D. Sontag, *Mathematical Control Theory*. Springer New York, 1998.